(ATINER)

Athens Journal of Sciences

(ATINER)

Volume 7, Issue 1, March 2020

Articles

Front Pages

ADEL RAZEK

The Observable, the Theory, and Prospective Revised Models for Societal Concerns

CECÍLIA BAPTISTA, NATÉRCIA SANTOS & MANUEL ROSA

Portuguese Hemp Plant as Raw Material for Papermaking

ABAYOMI AYOADE, ROTIMI FOLARANMI & TOLULOPE LATUNDE

Mathematical Analysis of the Implication of the Proposed Rise in the Retirement Age on the Unemployment Situation in Nigeria

SEBASTIAN STIGLER & MARINA BURDACK

A Practical Approach of Different Programming Techniques to Implement a Real-time Application using Django

Mission

ATINER is an Athens-based World Association of Academics and Researchers based in Athens. ATINER is an independent and non-profit **Association** with a **Mission** to become a forum where Academics and Researchers from all over the world can meet in Athens, exchange ideas on their research and discuss future developments in their disciplines, **as well as engage with professionals from other fields**. Athens was chosen because of its long history of academic gatherings, which go back thousands of years to *Plato's Academy* and *Aristotle's Lyceum*. Both these historic places are within walking distance from ATINER's downtown offices. Since antiquity, Athens was an open city. In the words of Pericles, **Athens*"...is open to the world, we never expel a foreigner from learning or seeing".*** **(**"Pericles' Funeral Oration", in Thucydides, *The History of the Peloponnesian War).* It is ATINER's **mission** to revive the glory of Ancient Athens by inviting the World Academic Community to the city, to learn from each other in an environment of freedom and respect for other people's opinions and beliefs. After all, the free expression of one's opinion formed the basis for the development of democracy, and Athens was its cradle. As it turned out, the Golden Age of Athens was in fact, the Golden Age of the Western Civilization. *Education* and *(Re)searching* for the 'truth' are the pillars of any free (democratic) society. This is the reason why *Education* and *Research* are the two core words in ATINER's name.

The Athens Journal of Sciences
ISSN NUMBER: 2241-8466- DOI: 10.30958/ajs
Volume 7, Issue 1, March 2020
Download the entire issue (PDF)

Front Pages i-viii

The Observable, the Theory, and Prospective Revised Models for Societal Concerns 1
Adel Razek

Portuguese Hemp Plant as Raw Material for Papermaking 15
Cecília Baptista, Natércia Santos & Manuel Rosa

Mathematical Analysis of the Implication of the Proposed Rise in the Retirement Age on the Unemployment Situation in Nigeria 29
Abayomi Ayoade, Rotimi Folaranmi & Tolulope Latunde

A Practical Approach of Different Programming Techniques to Implement a Real-time Application using Django 43
Sebastian Stigler & Marina Burdack

Athens Journal of Sciences
Editorial and Reviewers' Board

President's Message

All ATINER's publications including its e-journals are open access without any costs (submission, processing, publishing, open access paid by authors, open access paid by readers etc.) and is independent of presentations at any of the many small events (conferences, symposiums, forums, colloquiums, courses, roundtable discussions) organized by ATINER throughout the year and entail significant costs of participating. The intellectual property rights of the submitting papers remain with the author. Before you submit, please make sure your paper meets the basic academic standards, which includes proper English. Some articles will be selected from the numerous papers that have been presented at the various annual international academic conferences organized by the different divisions and units of the Athens Institute for Education and Research. The plethora of papers presented every year will enable the editorial board of each journal to select the best, and in so doing produce a top-quality academic journal. In addition to papers presented, ATINER will encourage the independent submission of papers to be evaluated for publication.

The current issue is the first of the seventh volume of the *Athens Journal of Sciences* (AJS) published by the Natural & Formal Sciences Division of ATINER.

Gregory T. Papanikos, President
Athens Institute for Education and Research

Athens Institute for Education and Research

A World Association of Academics and Researchers

8th Annual International Conference on Chemistry
20-23 July 2020, Athens, Greece

The Chemistry Unit of ATINER, will hold its **8th Annual International Conference on Chemistry, 20-23 July 2020, Athens, Greece** sponsored by the Athens Journal of Sciences. The aim of the conference is to bring together academics and researchers of all areas of chemistry and other related disciplines. You may participate as stream organizer, presenter of one paper, chair a session or observer. Please submit a proposal using the form available (https://www.atiner.gr/2020/FORM-CHE.doc).

Academic Members Responsible for the Conference

- **Dr. Ellene Tratras Contis**, Head, Chemistry Unit, ATINER & Professor of Chemistry, Eastern Michigan University, USA.
- **Dr. Nicolas Abatzoglou**, Head, Environment Unit, ATINER & Professor, Department of Chemical & Biotechnological Engineering, University of Sherbrook, Canada, Chair Pfizer, PAT in Pharmaceutical Engineering, Director GREEN-TPV and GRTP-C & Pwelcomes.

Important Dates

- Abstract Submission: **23 March 2020**
- Acceptance of Abstract: 4 Weeks after Submission
- Submission of Paper: **22 June 2020**

Social and Educational Program

The Social Program Emphasizes the Educational Aspect of the Academic Meetings of Atiner.

- Greek Night Entertainment (This is the official dinner of the conference)
- Athens Sightseeing: Old and New-An Educational Urban Walk
- Social Dinner
- Mycenae Visit
- Exploration of the Aegean Islands
- Delphi Visit
- Ancient Corinth and Cape Sounion

Conference Fees

Conference fees vary from 400€ to 2000€
Details can be found at: https://www.atiner.gr/2019fees

8th Annual International Conference on Physics
20-23 July 2020, Athens, Greece

The Physics Unit of ATINER, will hold its **7th Annual International Conference on Physics, 20-23 July 2020, Athens, Greece** sponsored by the Athens Journal of Sciences. The aim of the conference is to bring together academics and researchers of all areas of physics and other related disciplines. You may participate as stream organizer, presenter of one paper, chair a session or observer. Please submit a proposal using the form available (https://www.atiner.gr/2020/FORM-PHY.doc).

Important Dates

- Abstract Submission: **23 March 2020**
- Acceptance of Abstract: 4 Weeks after Submission
- Submission of Paper: **22 June 2020**

Academic Member Responsible for the Conference

- **Dr. Ethel Petrou**, Academic Member, ATINER & Professor and Chair, Department of Physics, Erie Community College-South, State University of New York, USA.
- **Dr. Bala Maheswaran**, Head, Electrical Engineering Unit, ATINER & Professor, Northeastern University, USA.

Social and Educational Program

The Social Program Emphasizes the Educational Aspect of the Academic Meetings of Atiner.

- Greek Night Entertainment (This is the official dinner of the conference)
- Athens Sightseeing: Old and New-An Educational Urban Walk
- Social Dinner
- Mycenae Visit
- Exploration of the Aegean Islands
- Delphi Visit
- Ancient Corinth and Cape Sounion

More information can be found here: https://www.atiner.gr/social-program

Conference Fees

Conference fees vary from 400€ to 2000€
Details can be found at: https://www.atiner.gr/2019fees

Athens Journal of Sciences 2020, 7(1): 1-14
https://doi.org/10.30958/ajs.7-1-1

The Observable, the Theory, and Prospective Revised Models for Societal Concerns

By Adel Razek[*]

Observational and modeling assessments involve many researchers in fundamental and applied investigations. This article attempts to shed light on these two concepts by underlining their specific uses in different branches of exploration. The nature of the field of research often involves observation, mathematical modeling or both concerns in the form of complementarity. In this work, we discuss for both concepts, the limits of their self-sufficiency. On the other hand, observation comes directly from reality and modeling comes from theory. In this article, we examine the circumstances of model approaches that reflect their intimacy with observed reality. In the case of such a reality corresponding to a societal application, the model often needs a reinforcement to advance towards its objective. A theoretical model generally concerns a given scientific field. In the meantime, the general model governing a societal application involves different theoretical domains. We study how to take into account these areas in the modeling of a given device for a particular environmental behavior. We discuss the choice of such a coupling strategy according to the degree of interdependence of the scientific domains involved. In several constituents of this work, we rely on neuroscience, social science and philosophical concepts. The contribution provides as well a typical application relative to the case of electromagnetic systems that involve magnetic, electrical, mechanical and thermal characteristics. We consider in such complex engineering case examples of different treatments of coupled models, related to different societal applications.

Keywords: *Observation, Modeling, Societal applications, Revisited models, Coupled modeling, Electromagnetic systems.*

Introduction

This contribution aims to investigate how observables and their models are close to each other and how the two issues of observation and modeling are codependent.

An observable real object behaves according to observable environmental events. We can define the model of such a real object as well as its environment, through the cause and effect of its observed behavior. Such an ascendancy is in generally relative to a science (physical, chemical, etc.) or to a phenomenon involved in a science (electromagnetic, mechanical, etc.).

We can carry on the analysis of a real object and its behavior according to real environmental events by observation and/or modeling. We can have an

[*]Emeritus Research Director, C.N.R.S. & Honorary Professor, CentraleSupelec, GeePs, University of Paris-Saclay and Sorbonne University, France.

interrogation on the self-sufficiency of each of these two issues of analysis as well as on their complementarity. The nature and field of investigation closely related to this questioning have specific considerations. Observation or modeling can be self-sufficient in areas of investigation that we often consider idealized. In the general case of real societal landscapes, we use the two issues of analysis in a framework of complementarity. Therefore, even in the domains calling usually for observation issue, this is in commonly not self-sufficient; (see for example, Lévi-Strauss 1958).

Also for the domains calling usually for modeling issue, this is in general not self-sufficient; (see for example, Merleau-Ponty 1960). Concerning the disagreement of a real observable and its model, we know that the first is correct (reference) and that it is necessary to revise the model to approach reality. Most of mathematical models originate of coherent and pleasant theories concerning one branch of science under idealizing assumptions concerning the environmental conditions such as temperature, pressure, etc., and the nature of materials such as homogeneity, viscosity, linearity, etc. In the real background of society, the environment and matter rarely meet such ideal conditions. In some special cases, we can take into account these imperfections by revising or adding specific coefficients. In the general case, the imperfections of the scientific branch implicated concern other scientific areas. Moreover, in certain societal panoramas, several branches of science may govern the behavior in question. In all these cases, the revised final model will be a coupled model resulting from the association of different theories of different scientific branches.

We often encounter such real societal applications. For example, we can take electromagnetic systems in general. The nature of the physical phenomena governing electromagnetic systems is complex and a complete model should take into account the magnetic, electrical, mechanical and/or thermal characteristics. The corresponding variables may be interdependent and the parameters may vary due to these variables. A physical model is, more or less coupled because of the importance of the interdependence of its related phenomena.

Observation Auto Sufficiency

We will consider first the domains of investigations that generally call for observation. A typical domain among these is Anthropology. We will consider an important field of this domain that is Myths. This field has used principally observation since its creation. This was mainly due to the richness of memory that is necessary for deep investigations in this field. In opposition, despite this richness of memory, the observation alone rapidly appeared limiting the extension of the field of research. Putting it in a theoretical context such types of investigations opens this field. Claude Lévi-Strauss (1908-2009) has illustrated this, in “Structural Anthropology”, Paris 1958, (see Lévi-Strauss 1958). He elucidated clearly in this work that structural researches in the social sciences are indirect consequences of modern mathematics: logic, sets, groups and topology. These theoretical "tools" make it possible to generalize a more in-depth research

involving different studied situations combined in the same model (theory). Consequently, these isolated observations may feed into a more general structured concept elucidating real universal phenomena. This example shows clearly that observation alone, even may be auto sufficient in certain situations, needs generally the modelling issue complementarity.

In physical science, we can consider a second example concerning the work of Michael Faraday (1791-1867) in the field of electromagnetic induction. Faraday was an excellent observer who transmitted his ideas resulting of his experimental work in a very simple style. His mathematical skills, however, are limited to the simplest algebra. The contributions of Faraday and others, to put them in a mathematical context and summarize them into a set of equations inspired James Clerk Maxwell (1831-1879). These “Maxwell equations” are the basis of all modern theories of electromagnetic phenomena and are the origin of many scientific research works in this area, as we will show in the last part of the present paper.

This complementarity (modeling helping observation) exists in many other areas of investigation in all fields of science, for example, demography, sociology, neuroscience, physical sciences.

Auto Sufficiency of Modeling

On the other hand, if we consider the areas of investigation that generally require modeling, for example physical, chemical, etc. In such cases, the establishment of coherent and pleasant theories (models) often requires assumptions simplifying or idealizing the real context of investigation. When the situation studied is very close to such an idealized context, the problem of modeling analysis could be self-sufficient. On the contrary, in most societal survey situations, this type of analysis will not be enough.

The great philosopher Maurice Merleau-Ponty (1908-1961) analyzed and commented on such situations in "The eye and the spirit", Paris 1960, (see Merleau-Ponty 1960). He observed, concerning isolated-use of theory, that science manipulates things, renounces living inside and considers the world as an object of knowledge "dissociated" from the existing subject. In addition, he added with regard to the models, that they are function of their authors, that there is correspondence between the model and the spirit, and that the scientists see the world with a spirit related to the model disregarding the reality observation. Therefore, theory cannot be used isolated of observation.

The Merleau-Ponty reflections suggest the existence of a correlation between the model, its author and the minds of its users. Nearly fifty years later, and thanks to research on modern neuroscience, the theory of mirror neurons has corroborated this suggestion. This work first showed for animals, then for humans, thanks to functional MRI brain mapping, that the zones of activated neuronal connections are similar, involving an observable and one or more observers, (see for example, Ferrari and Rizzolatti 2014).

It is interesting to note that, in general, one can consider a theory only

established after validation by observation. Moreover, such a theory remains valid until disagreement with observation. This shows the importance of observation in the foundation of science and therefore the theory-observation couple is necessarily always associated and the complementarity (modeling accounting for observation) exists in investigations in all fields of science.

Societal Scenery and Complementarity

From the analysis and discussion presented, it is obvious that in a typical societal application (real observable) in domains such as mobility, health, or security, we need a complete complementarity of the issues of observation and modeling. In fact, we know that the observable is reality and that the theoretical model is indispensable. When such a model does not correspond to the observable, we must revise it to bring it closer to the observable. One can consider this revision in the model in two different ways, either by approximation or by taking into account more theory in the model. Both approaches can lead to a better match of the observable and the model. In fact, approximation matching is often accidental and a bad option because "the adjustment is not necessarily tighter". Simplified models often correspond to non-universal approximations that incorrectly exercised for every one observable and can become dangerous through “recipes” operated in certain specialties. Therefore, we can only consider a correct revision in the model by taking into account more theory in such model.

Non-Universal Modeling Panoramas

As mentioned earlier, mathematical models come from coherent and pleasant theories under idealizing assumptions. When such theories apply to situations corresponding to these hypotheses, the model will represent reality; for example, in the case of electromagnetism, the conditions of infinitely small or large.

On the other hand, in the application of a complete theory on a situation in which a part (term) is negligible or non-existent; the corresponding approximate model will represent reality. For example, in the case of electromagnetism, we can neglect eddy currents in the modeling of nonconductive materials.

We cannot generalize the models considered in these two cases to the general cases of societal applications and in any case, we cannot consider them universal.

Revised Model Closer to the Observable

As mentioned earlier, if we consider the case of a model in an idealized context, the problem of modeling analysis could be self-sufficient. Considering a more realistic observable societal situation, the idealized model will not represent the behavior of the landscape. Only a revised augmented model involving more theory to account for the realistic aspect can represent such a panorama. The idealized context often corresponds to the disregarding of existing phenomena that governed by other branches of science. The augmented model must take into

account these additional occurrences. In fact, such a revised model corresponds to the processing of the idealized model associated with such surplus occurrences in a sort of mathematical cocktail. Because of this objective, we can consider such a treatment by systematic iterations between the mathematical models concerned by this cocktail. If these mathematical models are particularly interdependent and notably with complex behaviors laws, only a coupled solution of these models can give an image "closer to the observable" of this type of behavior.

Coupled Solution

The coupling of interdependent models could be weak, strong or intermediate. The degree of this interdependence corresponds directly to the degree of coupling required.

In the case of a weak coupling, one can consider the models individually in an iterative process involving their interdependent behavioral laws. We can call such case a weakly coupled (or a separately iterative coupled).

For the other limit of strong coupling, we must consider a simultaneous solution of mathematical models containing their behavioral laws. We can call this case a strongly coupled (or simultaneously coupled).

For a given degree of coupling the choice of, an appropriate mathematical formulation, suitable space and time scales and a correct resolution method can lead to the right behavior. In the general case, we use three-dimensional discretized geometrical cells or elements for the different space scales and a discretized form for the time. The degrees of discretization refinement of space and time depend on the complexity of the geometry, the nature of temporal evolutions of phenomena, and the individual and interdependent laws of behavior of variables.

Type of Exploration and Area of Expertise Requirements

Analysis and Reflection Depths

As stated earlier, we can approximate (idealize) the studied landscape or consider it completely in its real societal form.

In such idealized case, we are in the presence of a simplified model that the use obeys a given situation. In such a case, once we have chosen the model (as a tool), we do not need to think deeply and simply execute a sort of reflex.

In the second real societal case option, we need to consider an appropriate model. In such a case, we must properly examine the behavioral conditions of the scene and decide on the appropriate model respecting these conditions. In this case, we usually need a precise model of the coupled type. Unlike the idealized case (involving a reflex), it is necessary in this case more reflection (cogitation).

The two situations above (idealized and real), call for two completely different modes of thought (reflex and negotiation).

Again, thanks to research on modern neuroscience, the theory of neural plasticity clearly illustrates the difference between these two situations. Using functional MRI brain mapping, we can notice, for different situations requiring absolute concentration for a given action without any dispersion (no reflection), that complex multiple neuronal connections become extremely simple thanks to plasticity, (see for example, Adkins et al. 2006, Nielsen and Cohen 2008). We encounter such situations, for example in sports competitions where we need a very high level of concentration to achieve a precise action. We call this state "reflex state". This is the opposite state to that one where reflection maneuvering complex neuronal connections.

In case of deep reflection (cogitation or negotiation), the brain acts as a predictive system (Bayesian brain) operating in situations of uncertainty. Our reflection on the surrounding observables is not, established solely on the information of our perceptions. In its place, what we observe is, as well deeply transformed by the circumstance of our feeling and our prospects about it. The predictive model assumes that our brain generates sensory expectations at every moment and that only the error (difference between prediction and observation) exists in the transmitted neuronal discharges. In many areas of cognitive neuroscience, the Bayesian brain suggests a great capacity for statistical inference at several levels (perception, action, language, etc.); (see for example, Knill and Pouget 2004, Pouget et al. 2013, Amalric and Dehaene 2017).

Specialties of Modeling

The specialty (business) involving modeling-related activities could belong to different categories, from basic mathematical formulations to simple users of closed black box tools. We can classify these categories into two distinct professions. The first concerns the development and improvement of models with the aim of being as close as possible to the real observable landscapes. The second concerns the use of modeling tools. We can call the first developer and the second user. We can cite the following examples for these two professions: Developing a strong coupling tool (code) considering a simultaneous solution of mathematical models containing their behavioral laws is the occupation of a developer. The use of such a tool by a designer is the occupation of a user.

Developers are usually involved in experienced teams in applied mathematics, numerical analysis, computer science and the scientific fields concerned with the developed tool. It may be noted that, in such activity we meet general evolutions in the fields of, par example, computation capacity, algorithmic optimization, instrumentation, etc. The developers are supposed to work closely with the users.

These users must be experts in the tool specifications and involved in the teams working in the heart of societal sceneries. By definition, a user far from either the tool or the societal domain could be hazardous. It is notable that, rapid technological developments and fields that are more specific generally characterize societal sceneries.

Case of Electromagnetic Systems (Application)

Introduction

Electromagnetic systems are present in most of societal applications: mobility, health, security, communication …These systems behave under four occurrences: electrical, magnetic, mechanical, and thermal. In electromagnetic systems, we need generally to consider the coupling of the magnetic field with the other occurrences. Among the concerned couplings, one is integrated (electrical and magnetic), while the others are causative; (see Piriou and Razek 1993, Ren and Razek 1994, Piriou and Razek 1990, Ren and Razek 1990, Sekkak et al. 1994, Sekkak et al. 1995).

The first three occurrences have relatively rapid time evolutions (small time-constants). The forth one (thermal) has a slower time evolution (higher time-constant). Moreover, apart from the classification of integrated and causative occurrences, we have the case of material intrinsic manifestations. This concerns mainly smart materials where the functioning involves two of these occurrences; for example, the case of piezoelectric materials that the functioning calls electrical and mechanical (deformation) behaviors. As well as, the case of magnetostrictive materials, that involve magnetic and mechanical (deformation) in their functioning. It is noteworthy that in electromagnetic smart systems that involve such smart materials, we may have a mixture of occurrences: integrated, causative, and/or material intrinsic.

In the general case, the determination of the system behavior for a given functioning, needs the solution of the equations of the involved governing occurrences. As the system structures are generally of complex geometry and involving materials with non-linear behavior laws, we need the local distribution of variables. Due to this, we use 2D or 3D discretized geometrical cells or elements to obtain the local solution of the needed variables. On the other hand, the nature of the concerned system behavior implies either a frequency domain analysis or a time domain analysis (discretized form of the time). The degrees of discretization refinement of space and time depend on the complexity of the geometry, the nature of temporal evolutions of phenomena, and the individual and interdependent laws of behavior of variables.

In the general case, for structures affected by independent occurrences with very different time constants (very different time evolutions) and involving, a material that behaves linearly, we need a simple weak coupling solution (direct separate solutions). However, if the material behaves non-linearly and/or the involved variables are interdependent, the weak coupling will be separately iterative.

In the contrary, in the case of occurrences with the same order of time constants (near time evolutions) and materials with non-linear behavior; we need a simultaneous strong solution. The non-linearity, as well as the variables interdependence, are included in the simultaneous solution through iterative convergence procedure

Therefore, for devices affected by two or more characteristics (occurrences)

of those three with small time-constant, we need generally a strong coupling (simultaneously coupled) except the case of linear behavior; (see for example, Piriou and Razek 1993, Ren and Razek 1994). For those concerned by two occurrences including the thermal one, we can use a weak separately iterative coupling; (see for example, Sekkak et al. 1994, Sekkak et al. 1995). We will consider in the following examples these two cases.

Electromagnetic Integrated Interaction

An electromagnetic system is composed of an electrical circuit and a magnetic circuit. These two circuits are essentially independent in their construction but not in their design. Therefore, we must consider the electrical circuit when exploring electromagnetic systems. A weakly coupled model does not represent reality in the general case. The solution of the problem depends on the laws of behavior and the topologies of these circuits. In the case of linear circuits, weak coupling of electrical and magnetic circuits can be used (Piriou and Razek 1990). In the case of nonlinear magnetic or electrical circuits, only a strongly coupled (simultaneous solution) model can be used (Piriou and Razek 1993). On the other hand, considering the topological aspect, in the analysis of electromagnetic structures simultaneously considering the magnetic and electrical equations (strong coupling), many works have been exposed in the 2D case; (see for example, Ancelle et al. 1980, Nakata and Takahashi 1986, Konrad 1981, Shen et al. 1985, Pawlak and Nehl 1988). Generally, in such a case one solves the magnetic equations by means of a formulation with the magnetic vector potential. The coupling is achieved through the conductor current expressed in terms of current density and the flux linkage expressed from the vector potential. In the case of 3D geometries, different formulations can be used according to the studied problem. The problem could be magnetostatic or magnetodynamic (involving eddy currents). The analysis could be in the frequency domain or the time domain. In Piriou and Razek (1993), the problem of strong coupling of magnetic and electric equations is analyzed in its general form. A 3D (or 2D) model for time domain finite element analysis based on the simultaneous solution of non-linear (or linear) magnetic and electric equations is presented and illustrated by several application concerning different devices.

Magneto Mechanical Causative Interaction

We consider the case of magneto mechanical interaction. In electromagnetic devices, the magnetic materials are subject to an elastic deformation under the charge of magnetic forces. In reverse, the magnetic field and the force distributions are, more or less influenced by the deformation. The study of such an interaction needs a simultaneous consideration of magnetic and mechanical fields. The degrees of coupling are different according to the significance of the interaction. For example in electrical machines, the deformation generated by magnetic forces is generally small and the variation of the magnetic field distribution is negligible. In such case, we can solve the magnetic and mechanical problems separately

(weak coupling); (see for example, Ren and Razek 1990). However, in other applications, for example magnetic forming, the deformation (or the displacement) is essential and modify the magnetic field and therefore the magnetic force distribution. This change is due to two facts: The first is the change of mechanical structure. The second is the change of magnetic permeability with mechanical stress (magnetostriction). Such case corresponds to strongly combined magnetic and mechanical phenomena and so we need to use a strong-coupled model (Ren and Razek 1994).

Magneto Thermal Causative Interaction

Concerning magneto thermal coupling, we can consider a specific medical application relating to hyperthermia techniques in the treatment of cancer (Sekkak et al. 1995). In this case, the thermal behavior is very slow (high time constant) with respect to this of the electromagnetic radiation (very low time constant). In such a case, we can solve separately the two governing equations in an iterative process (weak coupling). Therefore, when studying the potential of such techniques, it is possible to calculate the temperature distribution in biological tissues produced by electromagnetic radiation that is determined separately. With this objective, it is possible to use a three-dimensional thermo-electromagnetic model for the analysis of high-frequency electromagnetic heating of biological bodies. The accumulation of electromagnetic energy is determined using three-dimensional local field computations. One can compute the local thermal distribution from the generated thermal power with a three-dimensional model. In these calculations, we can use a dielectric material with losses whose physical parameters are those of biological tissues (such as fat and muscle).

Material Intrinsic Interactions

As mentioned before, the case of smart materials that their functioning uses properties of the basic four occurrences, needs the consideration of coupling. The study of such an interaction needs a simultaneous consideration. The degree of such coupling depends on the time constant of the phenomena as well as the laws of behavior of the material. In case of material linear behavior and/or very different time constants of phenomena, we can use a weakly coupled solution. Otherwise, we need a strong coupling.

Considering the case of piezoelectric (electrostrictive) materials that present a linear behavior, the solution involves a weak coupling of electrical and mechanical deformation. In such case, the presence of an electric field produces a deformation (direct effect) and the application of a stress induces an electric potential (inverse effect). We can use the benefit of these properties for sensor, actuator or electric source applications.

In reverse, the case of magnetostrictive materials that behaves non-linearly, we need a simultaneous strong coupling. Different applications use magnetostrictive materials that present magnetic and mechanical properties, which are strongly coupled. In such case, the presence of a magnetic field produces a deformation

(magnetostriction strain or direct effect) and the application of a stress induces a magnetization of the material (inverse effect). It may be noted that, in the direct effect the magnetic field causes elastic deformation or variation of the Young's modulus, and in the inverse effect the mechanical stress modifies the magnetic properties: the magnetization curve (function) or the hysteresis loop. These two effects have been found separately. Joule discovered the direct effect in 1842. Two decades later, Villari exposed in 1864 that the stresses have an impact on the magnetization that do the sign of the deformation of the material govern by magnetostriction. Posterior, it was acknowledged that these two occurrences link to the same thermodynamic relation. It is worth notable that, it is recalcitrant to characterize magnetostriction-strains from measurements. This is not only for the reason that their amplitude is insignificant, but also for the reason that they strongly depend on texture, material constitution, and the applied stresses. The measured deformations outcome from unattached processes: pure magnetostriction strains and elastic deformations due to magnetic forces.

We can use the benefit of magnetostrictive materials properties for sensor and actuator applications. In addition, the magnetostrictive property besides being beneficial in such cases, for example, in ultrasonic applications, it could also present some undesirable effects in other applications. For example, the generation of acoustic noise in electromagnetic power systems (transformers, electric machines, etc.).

In the case of material intrinsic interactions, one may use different means for the modelling of the magneto elastic effects, depending on the preferred scale level of description. Such a choice depends on the need for investigation in terms of analysis, design or optimization. This may concern more precisely materials that magneto elastic intrinsic interaction corresponds to their self-functioning. For example, the quest for materials styled to specific applications e.g. transducers, calls for the use of well along constitutive models, accounting for coupled magneto-mechanical phenomena involved in such applications. One can consider more specifically typified the magneto-mechanical coupling in this case, by the stimulus of stress on the magnetic susceptibility (supporting the effective consequence of stress on the functioning of such devices) and by the magnetostriction (exploited in magnetostrictive transducers).

On the macroscopic scale, the two phenomena of the direct and inverse effects of magnetostriction, mentioned in the last section illustrate the coupling between the elastic and magnetic behaviors of ferromagnetic materials. The complexity of the nonlinear relationships of these phenomena is such that, it seems difficult to propose realistic macroscopic behavioral equations to model the coupled magneto-elastic behavior of magnetic materials. In other words, magnetostriction and magnetization are macroscopic manifestations of the complex structure of the magnetic domains that modified by the applied mechanical and magnetic loads.

In microscopic methodologies, we can define the structure at the atomic level and the materialization of magnetic domains may be the result of atomic interactions. The outcomes sent by such representations are intimate to physical observations, but they call for expensive computations whose extension is

problematic up to a macroscopic scale.

On the other hand, for macroscopic approaches, we can study the material as a continuum and thus we can define its condition by some evaluable and internal variables such as magnetization, magnetostriction strain and supposedly irreversible magnetization. One can use thermodynamic relations to derive complete constitutive relations. The calculation times may be low, but the structure of the magnetic domain is not involved. It is therefore, as mentioned before, difficult to describe with such one-scale model the couplings between the different variables and their evolution as well as phenomena occurring for complex loadings.

Different solutions accounting for both microscopic and macroscopic aspects based on specific assumptions and approximations permit to obtain material constitutive models, accounting for coupled magneto-mechanical phenomena; (see for example, Besbes et al. 2001, Buiron et al. 1999, Daniel and Galopin 2008).

A joint analysis of the magnetic and mechanical phenomena taking into account the magnetostrictive property requiring the use of a strongly coupled model is given in Besbes et al. (2001). This work considers the equations that govern the magneto-elastic phenomena associated with their boundary conditions and their laws of behavior. It presents the different forms of energy in a magnetostrictive material. An investigation of three cases of constitutive laws of behavior: the linear case, the nonlinear magnetic with linear elastic case, and the all-nonlinear case, is carried out. The energy functional corresponding to each case is developed. By minimizing the total functional energy, a local distribution of variables model of the problem in terms of magnetic vector potential and displacement is obtained. An example studied in this article illustrates the interaction phenomena between magnetic and elastic properties. This is clearly demonstrated through the modification of the distribution of the force and the deformation with respect to the situation without taking into account the magnetostrictive force.

In a kind of micro-macro or multiscale methodologies, Buiron et al. (1999) propose to use homogenization techniques to realize the macroscopic behavior of single crystals and polycrystals from a statistical picture of the magnetic domain structure. So, one can determine global values of magnetostriction strains. Therefore, the macroscopic couplings naturally get up from the expression of the free energy expressed at the level of the magnetic domains. Computation are longer than for macroscopic models, but more information can be determined from the microscopic scale (domain structure, texture, anisotropy) and the modelling of couplings between phenomena is generally simplified because expressed at a lower scale. In an application of the multiscale approach for magnetostrictive behavior modeling, Daniel and Galopin (2008) present, based on a statistical energetic description of the domain microstructure evolution, an analysis in the case of anhysteretic behavior, of the case of Terfenol-D single crystals and polycrystals.

Conclusions

This paper endeavors to examine the two concepts of observational and mathematical modeling assessments by highlighting their specific uses in different branches of scientific exploration. We discussed the nature of the research domains involving observation, mathematical modeling, or both concerns. We explore the circumstances of model approaches that reflect their intimacy with observed reality. We have shown that in the case of such a reality corresponding to a societal application, the model often needs a reinforcement to advance towards its objective. We study how to take into account, in the model governing a societal application, the different theoretical domains involved in the modeling of a given device for a particular environmental behavior. We discuss the choice of such a coupling strategy according to the degree of interdependence of the scientific domains involved.

The contribution provides examples of different applications of coupled models in the case of electrical engineering (electromagnetic systems), related to different societal applications. In this case, we illustrated the need to consider the different behaviors involved in electromagnetic systems: electrical, magnetic, mechanical and thermal. The associations of these behaviors in weak or strong couplings clearly illustrate the concept of the model revisited to get closer to the observable reality (Razek 2017).

As general conclusions, first for the self-sufficiency of observation and modeling we can settle that both, except for particular cases, are complementary and materialize an associated couple. The observation needs modeling to permit a necessary generalizing context for outspread research. The model needs observation to verify its validity and to reinforce its nature to meet the observed reality. As a second conclusion, the observable is real and the model needs revision to match the observable. We can do such revision by associating the other theories corresponding to phenomena involved in the societal application. The revised model results from coupling of such associated models. The degree of coupling depends on the interdependence of the involved phenomena and the concerned behavior laws. The more, interdependent are the phenomena and nonlinear are the behavior laws, stronger will be the coupling (simultaneous solution of equations). In the contrary case, we need weaker coupling (direct or separate solution of equations). The third point concerns the developer and the users of the revised models. Developers are supposed to be engaged in skillful teams in applied mathematics, numerical analysis, computer science and the scientific fields relate to the developed tool; they are expected to work closely with the users. These users must be experts in the tool stipulations and implicated in the teams working in the heart of societal sceneries.

References

Adkins DL, Boychuk J, Remple MS, Kleim JA (2006) Motor training induces experience-specific patterns of plasticity across motor cortex and spinal cord. *Journal of Applied Physiology* 101(6): 1776-1782.

Amalric M, Dehaene S (2017) Cortical circuits for mathematical knowledge- Evidence for a major subdivision within the brain's semantic networks. *Philosophical Transactions of the Royal Society B - Biological Sciences* 373(1740): 20160515.

Ancelle B, Coulomb J, Morel B, Belbel E (1980) Implementation of a computer aided design system for electromagnet in an industrial environment. *IEEE Transactions on Magnetics* 16(5): 806-808.

Besbes M, Ren Z, Razek A (2001) A generalized finite element model of magnetostriction phenomena. *IEEE Transactions on Magnetics* 37(5): 3324-3328.

Buiron N, Hirsinger L, Billardon R (1999) A multiscale model for magneto-elastic couplings. *Journal Physics* 9(PR9): 187-196.

Daniel L, Galopin N (2008) A constitutive law for magnetostrictive materials and its application to Terfenol-D single and polycrystals. *The European Physical Journal - Applied Physics* 42(2): 153-159.

Ferrari PF and Rizzolatti G (2014): Mirror neuron research - the past and the future. *Philosophical Transactions of the Royal Society of London. Series B, Biological Sciences* 369(1644): 20130169.

Knill DC, Pouget A (2004) The Bayesian brain: the role of uncertainty in neural coding and computation. *Trends in Neurosciences* 27(12): 712-719.

Konrad A (1981) The numerical solution of steady-state skin effect problems - an integrodifferential approach. *IEEE Transactions on Magnetics* 17(1): 1148-1152.

Lévi-Strauss C (1958) *Structural anthropology*. Paris.

Merleau-Ponty M (1960) *The eye and the spirit*. Paris.

Nakata T, Takahashi, N (1986) Numerical analysis of transient magnetic field in capacitor-discharge impulse magnetizer. *IEEE Transactions on Magnetics* 22(5): 526-528.

Nielsen JB, Cohen LG (2008) The Olympic brain. Does corticospinal plasticity play a role in acquisition of skills required for high-performance sports? *The Journal of Physiology* 586(1): 65-70.

Pawlak AM, Nehl TW (1988) Transient finite element modelling of solenoid actuators: the coupled power electronics mechanic and magnetic field problem. *IEEE Transactions on Magnetics* 24(1): 270-273.

Piriou F, Razek A (1990) Numerical simulation of a nonconventional alternator connected to a rectifier. *IEEE Transactions on Energy Conversion* 5(3): 512-518.

Piriou F, Razek A (1993) Finite element analysis in electromagnetic systems accounting for electric circuits. *IEEE Transactions on Magnetics* 29(2): 1669-1675.

Pouget A, Beck JM, Ma WJ, Latham PE (2013) Probabilistic brains: knowns and unknowns. *Nature Neuroscience* 16(9): 1170-1178.

Razek A (2017) *For contributions to coupled multiphysics modeling and design of electromagnetic systems*. https://www.ieee.org/about/awards/bios/tesla-recipients.html, IEEE_Nikola_Tesla_Award-2017.pdf.

Ren Z, Razek A (1990) A coupled electromagnetic - mechanical model for thin conductive plate deflection analysis. *IEEE Transactions on Magnetics* 26(5): 1650-1652.

Ren Z, Razek A (1994) A strong coupled model for analyzing dynamic behaviors of non-linear electromechanical systems, *IEEE Transactions on Magnetics* 30(5): 3252-3255.

Sekkak A, Pichon L, Razek A (1994) 3-D FEM magneto-thermal analysis in microwave ovens. *IEEE Transactions on Magnetics* 30(5): 3347-3350.

Sekkak A, Kanellopoulos VN, Pichon L, Razek A (1995) A thermal and electromagnetic analysis in biological objects using 3D finite elements and absorbing boundary conditions. *IEEE Transactions on Magnetics* 31(3): 1865-1868.

Shen D, Meunier G, Coulomb J, Sabonnadiere J (1985) Solution of magnetic field and electrical circuit combined problem. *IEEE Transactions on Magnetics* 21(6): 2288-2291.

Athens Journal of Sciences 2020, 7(1): 15-28
https://doi.org/10.30958/ajs.7-1-2

Portuguese Hemp Plant as Raw Material for Papermaking

By Cecília Baptista[‡], Natércia Santos[±] & Manuel Rosa[*]

The objectives of this study were the physical and chemical characterization of Portuguese industrial hemp and the assessment of its suitability to produce kraft pulp. A comparison was established with a reference eucalyptus pulp, obtained by the same chemical process. Handmade paper sheets were prepared in the laboratory using hemp pulp, eucalyptus pulp and a blend of both fibres in order to compare final paper properties. The unbleached pulp was produced by batch kraft cooking (NaOH + Na_2S) and the evaluation of pulp bleachability was carried out under a $D_0E_0D_1E_1D_2$ sequence. The physical properties of laboratory papers prepared with different compositions (100% hemp, 100% eucalyptus, hemp/eucalyptus 50:50) were assessed according to International Standards. Hemp fibres present two fractions, bast and core (33% and 67% of the total stem mass, respectively) with distinct biometric characteristics and cell composition. The hemp plant allowed cooking yield overlapping the wood reference, with lesser uncooked fractions. The pulp exhibited a good bleachability, even better than the reference. Hemp plant allowed a pulp with a higher gain of brightness and lower loss of intrinsic viscosity than eucalyptus. Hemp pulp also showed a better beatability, superiority in tearing resistance and a lower air permeability. The paper sheets obtained with the hemp/ eucalyptus mixture showed interesting properties, which predicts a suitable combination of these two raw materials for papermaking.

Keywords: *Bleachability, Hemp plant, Kraft cooking, Papermaking, Physical properties.*

Introduction

Hemp (*Cannabis sativa* L. var. sativa) is a non-woody plant originated from Central Asia (Hillig 2005), farmed worldwide and having a wide variety of applications, namely in food, cosmetics, construction, textile and paper industries. Actually, the largest European producer is France, where the main destination is the production of special papers; China is also an important producer (Bouloc et al. 2013, Amaducci et al. 2015).

There are many scientific studies focusing hemp in general, its chemical composition, physical and chemical characteristics, pulping and bleaching aptitude, potential as a reinforcing fibre with hardwood and softwood fibres (Aitken et al. 1988, Malachowska et al. 2015, Danielewicz and Surma-Ślusarska 2017, Danielewicz and Surma-Ślusarska 2019a). Different hemp plants from particular

[‡]Professor, Polytechnic Institute of Tomar, Portugal.
[±] Professor, Polytechnic Institute of Tomar, Portugal.
[*]Professor, Polytechnic Institute of Tomar, Portugal.

regions were studied, mainly from Canada, Eastern Europe, Asia and Australia, but there are few studies on the Portuguese hemp or industrial hemp farmed in similar geoclimatic regions (Wong and Chiu 1995, Correia et al. 1998, Barberà et al. 2011). The plant is strongly affected by the climate and soil and, thus, the obtained results can be somewhat different. Hemp plant exhibits in the stalk two distinct regions and usually this feature implies an initial stem processing in order to separate both fractions. Most of the studies present the pulping results from these two isolated fractions.

Non-woody plants have been used in papermaking for several reasons. One of the most relevant motives is the reduction of wood dependence which became an increasing problem for paper industry in recent decades. Other reasons concern the technological process involved, once this raw material possess an interesting chemical composition (high polysaccharide and low lignin contents) allowing the improvement of some pulping and bleaching process variables and some paper properties, as well as, the reduction of chemical reactant needs and beating energy consumption. Among the most non-woody plants used for papermaking one can refer cereal straw, sugarcane bagasse, bamboo, sisal, abaca, kenaf, cotton, and hemp. Industrial hemp has been used for pulp production and as reinforcing fibres for hardwood kraft pulps (Correia et al. 2003, Danielewicz et al. 2018). Furthermore, this plant can be fractionated in different biorefinery approaches (Johnson 1999, Danielewicz and Surma-Ślusarska 2010, Lavoie and Beauchet 2012, Malachowska et al. 2015). Some studies use hemp plant in blend with other pulp and paper raw materials, such as pine and birch, to obtain bleached pulp, and the results were promising (Danielewicz and Surma-Ślusarska 2019a, Danielewicz and Surma-Ślusarska 2019b).

This plant was farmed in Portugal from the 14th to the 20th century to produce fibres for cloths and ropes. The tows were used for papermaking, for instance, the cigarette paper produced at the Matrena paper mill in Tomar (Portugal). Since the 1970's, the synthetic fibres development caused the loss of market competitiveness of this raw material for the textile industry. The seasonality of crops and the stems processing, which require specific equipment to separate bast and core fibres, impose some limitations on this production. However, from the 90's of the 20th century, the demand and the interest for its farming increased (Salentijna et al. 2015, Schluttenhofer and Yuan 2017), since this species is suitable for different climatic conditions, from the regions of temperate climate to areas of boreal climate (Pahkala et al. 2008).

In recent years there has been some interest in Portugal for the cultivation of industrial hemp for different purposes, from the food industry to the textile industry, but producers have encountered some difficulties due to the need for initial processing to separate the fibres from the outer and inner zone of the stems.

In the present research, the whole hemp stem was used to avoid the cost of initial processing and to allow the possibility of using the current wood chips cooking technology. Replacing wood kraft fibres with kraft fibres of whole hemp stem in papermaking would be the advantage of the industrial application of this study.

This work aims to characterize the industrial hemp produced in Portugal

(moderate Atlantic and Mediterranean climate area) and to assess the paper potential using the whole stalk, which avoids the use of specific equipment to sort bast and core fibres. The hemp plant was used in the conventional kraft cooking process without retting or decortication. The bleachability and beatability of the unbleached pulp were also studied. A systematic comparison was made with a conventional eucalyptus pulp and an equitable blend was produced with these two pulps (hemp and eucalyptus) in order to obtain a paper with the contribution of both fibres' intrinsic properties.

Materials and Methods

Raw Material

The hemp plant used in this study was produced in Mora (Alentejo) and was supplied as whole stems. The stems were washed with water, dried and cut with scissors into pieces of 2-3 cm length. The eucalyptus wood, in the form of industrial chips, was used as the reference raw material.

Morphological and Chemical Characterization

The stems pieces were cut with a length of approximately 1 cm and therefore distinguished in two different zones (the inner zone, woody-core fibres, and the outer zone, bast fibres) in order to analyse separately their morphology. A fraction of 1 g of each fibre was macerated in an oven (55 °C), during 48 h, in a 30 mL solution of hydrogen peroxide and glacial acetic acid (1:1). The solvent was renewed, and the maceration was repeated for a further period of 48 h. After stirring with a glass rod, the dissociated vegetable material was filtered through a crucible (porosity 2) and washed with boiling distilled water, until reach a neutral pH. An Olympus CH30RF200 optical microscope was used in the morphological characterization and the biometric analysis was carried out in a Morfi V7 9.5 analyser.

The stems were ground in a Retsch SM1 mill and the sawdust was classified in an Endecotts Octagon 200 sieve. The characterization was performed with the fraction retained in the 60-mesh screen. Two distinct texture fractions were identified in the sieving process; one of them was grainier (the core fraction) and the other one was fluffier (the bast fraction). A classical chemical characterization of the whole stem was carried out to determine the main chemical constituents after extraction of the material with ethanol/toluene (1:2). All the processes were carried out at least in duplicate and according to the following standards: Sampling and preparing wood for analysis - TAPPI 257 cm-85; Preparation of wood for chemical analysis - TAPPI 264 cm-97; Ash in wood, pulp and paperboard: combustion at 525 ºC - TAPPI 211 om-93; Solvent extractives of wood and pulp - TAPPI 204 cm-97; Acid-insoluble lignin in wood and pulp - TAPPI T 222 om-02; Acid-soluble lignin in wood and pulp - TAPPI UM 250-85; Holocellulose content - peracetic acid method and Cellulose content - Kürschner and Hoffer method. A

DR Lange Cadas 100 spectrophotometer was used for the determination of soluble lignin. For further calculations, cellulose and lignin fractions from the holocellulose were determined, as well as, the ash content of insoluble lignin.

Raw Materials Cooking

The cooking liquor was prepared by dissolving NaOH and Na_2S in water and the cooking was carried out under the following operating conditions: active alkali - 22%; sulfidity - 30%; maximum temperature – 160 °C; time until the maximum temperature is reached - 90 min; time at the isothermal maximum temperature - 120 min; liquid-to-wood ratio - eucalyptus - 5:1 and hemp - 7:1. The reagents used for pulping were of high purity grade purchased from Sigma-Aldrich and Riedel-de Haën. The cooking was performed in a batch reactor "Haato-tuote oy" of 10 dm^3.

The hemp pulping was performed with the entire stems (including bast and core), broken into pieces of 2-3 cm long.

After the end of the pulping time, the pressure in the digester was released and the cooked material was transferred to a three sequential screen device. The first filtration step occurred on a 64-mesh metallic screen for disaggregation of the cooked chips under water pressure while the second was carried out on a 400-mesh metallic screen that retains the washed fibres. The third screening level was performed on a double layer polyester wire with 2500-mesh, approximately, in order to retain the fines. The fibres and fines from the second and third filters were collected, remixed and dewatered before drying at room temperature.

The Portuguese Standard NP 3186:1995 was used for the determination of the kappa number, weighing about 2 g of eucalyptus pulp and 1 g of hemp pulp.

The determination of the intrinsic viscosity of the pulp followed the ISO Standard 5351/1: 1981, Part 1, Alternative A, using 0.05 g of cellulosic fibres (o.d.). The cellulose polymerization degree (DP) was calculated by equation (1), where [η] is the pulp intrinsic viscosity value.

$$DP^{0,905} = 0,75 \times [\eta] \quad (1)$$

Pulp Bleaching

The unbleached pulps were bleached in an ECF (Elemental Chlorine Free) sequence of the type $D_0E_0D_1E_1D_2$. The oxidizing reagent (D) used was chlorine dioxide (ClO_2). The oxidation reaction occurred in acidic medium followed by an alkaline extraction (E) with NaOH to remove previously oxidized lignin fragments. All bleaching tests were performed with 6 replicates and a dry fibre mass of 10 g. During the tests, both pulps were subjected to the same conditions, differing only in the ClO_2 and NaOH amount used because they depended on the kappa number (KN) of the raw pulp. Steps D and E were carried out in plastic bags, kept in thermostatic water bath at 70 ºC. Initial pH control was performed with the pH meter and the necessary adjustments were carried out with the addition of 0.1M HCl. The bags contents were manually homogenized at 15 minutes intervals and

the operating conditions are shown in Table 1. The bleaching agent ClO_2 was prepared in the laboratory by the reaction between $NaClO_2$ and concentrated H_2SO_4, and subsequent absorption of the released gas in distilled water at 5-7 ºC. The bleaching active agent (Cl_2) concentration in the prepared solution was determined by titration with a 0.1M $Na_2S_2O_3$ solution.

Table 1. *Operating Conditions and Chemical Charges Applied during Bleaching*

Conditions	**D_0**	**E_0**	**D_1**	**E_1**	**D_2**
Consistency (%)	10	10	10	10	10
Time (min.)	90	60	120	60	120
pH	2	11	4	11	4
Charge (%)	0.25KN/2.63	0.5 Cl_2 active D_0 + 0.15	1.5 Cl_2 active	1.0%	0.5 Cl_2 active

Properties of Paper Samples

Three samples of unbleached pulps were studied: hemp pulp, eucalyptus pulp and hemp/eucalyptus blend pulp 50:50.

Before the beating process, the two pulps were disintegrated using the British Pulp Evaluation Apparatus disintegrator according to ISO standard 5263:2004. Initially, the beatability of each pulp was assessed through the refining curves. Subsequently, 30 g of each pulp were refined in a laboratory refiner to reach a beating degree, performed in a beating and freeness tester – Schopper-Riegler type, between 35 and 40 ºSR in order to produce 12 handsheets for each fibre composition. The handsheets were made according to TAPPI Standard sp 205-02 in a Lorentzen & Wettre handsheet former (TAPPI type) using standard stirrer and couch roller. The design of the drainage system of this device provides a uniform flow across the entire wire, thus permitting uniform sheets. Laboratory sheets with 200 cm^2, prepared from the different pulp's suspensions were used for later physical properties determination. The handsheets goal basis weight was 60 g/m^2 and the sheet set was pressed in a AB Lorentzen & Wettre pneumatic press. Finally, handsheets were air-dried in accordance with the standard previously referred, using standard drying plates and rings.

Paper properties assessment was carried out, according to international standards for two types of tests, namely *i)* - *structural properties*: Thickness and Bulk - ISO 534:1988 Paper and board -- Determination of thickness and apparent bulk density or apparent sheet density; Bendtsen Roughness - ISO 8791-2:1990 Paper and board -- Determination of roughness/smoothness (air leak methods) -- Part 2: Bendtsen method; Bendtsen Air permeability - ISO 5636-3:1992 Paper and board -- Determination of air permeance (medium range) -- Part 3: Bendtsen method and *ii)* - *strength properties*: Tensile strength and stretch - ISO 1924-2:2008 Paper and board -- Determination of tensile properties -- Part 2: Constant rate of elongation method (20 mm/min); Tearing resistance - ISO 1974:2012 Paper -- Determination of tearing resistance -- Elmendorf method. These properties were evaluated using the three fibrous compositions handsheets.

In the bleachability study, pulps reflectance and ISO Brightness were

measured according to ISO 2470-1:2016 Paper, board and pulps — Measurement of diffuse blue reflectance factor — Part 1: Indoor daylight conditions (ISO brightness) using the Elrepho 0.7 colorimeter.

Results and Discussion

Morphological and Chemical Characterization

The morphological analysis gave rise to several microphotographs of the two different types of fibres and other plant cell elements, as depicted in Figure 1.

Figure 1. *Microphotographs of Hemp Fibres (Gx 100): A) Bast Fibres of the Stem Outer Zone - (1) Nodes and (2) Tapering Tips; B) Core Fibres of the Stem Inner Zone - (1) Vessel Elements and (2) Agglomerated Short Fibres*

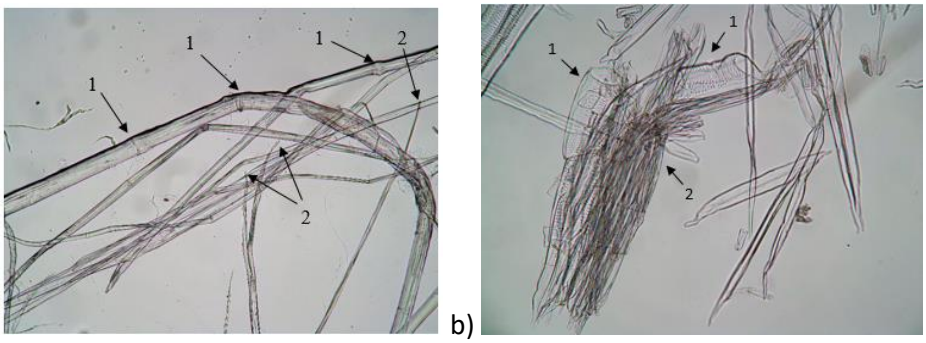

The morphological analysis showed the two main types of fibres, the phloem (long) and xylem fibres (short), as it can be observed in Figure 1. Other cell types, namely vessel elements and wood fibres, are visible in the inner zone. In Figure 1a, it is possible to observe the rounded section of fibres and identify some nodes (1), typical and very common in hemp and linen lignified fibres. The fibres do not exhibit any twisted zones, as expected for this non-woody raw material, allowing an easy distinction from cotton. Besides most of the fibres are longer than the microscope image field, one can observe some tapering tips (2) in the smallest ones. The wood or xylem cells present different diameter vessel elements (Figure 1b) which show open perforation plates and multiple pitting. The clustered elements indicate a dissociation process which was not taken to limit.

Table 2 displays the results of the biometric characterization of hemp fibres. Bast fibre parameters were determined using four samples with a global number of 543484 counted objects. Core fibre parameters were determined using three samples making up a total number of 662701 counted objects.

Table 2. *Biometric Parameters of Hemp Fibres*

Parameters	**Bast fibres (mean value ± s.d.)**	**Core fibres (mean value ± s.d.)**
Length (mm)	1.28 ± 0.12	0.46 ± 0.01
Width (μm)	25.1 ± 0.97	26.9 ± 0.05
Kink (°)	115 ± 1.00	113 ± 0.50
Kinked fibres (%)	46.8 ± 2.56	6.0 ± 0.17
Curl (%)	12.3 ± 0.27	3.5 ± 0
Broken ends (%)	56.5 ± 5.81	26.6 ± 0.21

Bast fibres are much longer (Lm = 1.28 mm) than the core fibres (Lm = 0.46 mm), showing a length, at least, three times bigger than the core ones, although the obtained value may have been influenced by the cut imposed prior to the stem's dissociation. This cut also highly affects the standard deviation founded for the content of twisted fibres and broken ends. Eucalyptus has an average fibre length between hemp bast and core fibres (Foelkel and Zvinakevicius 1980). Despite the different length, the kink angles are similar varying between 112° and 116°.The widths (lm) exhibited by the two types of fibres are more identical, lm = 25.1 μm and lm = 26.9 μm, respectively, for bast and core fibres, in accordance to the literature reference, lm = 25 μm, (Aitken et al. 1988). The percentage of kinked fibres, curl and broken ends are biometric parameters very different between bast and core fibres. The percentage of kinked bast fibres is eight times superior, while the curl is almost four times higher, which is certainly due to the smaller size of these latter cells, and consequently, less tendency to wind.

The chemical composition of the two individualized fractions was determined, as well as, the whole stem composition, reconstituted according to the experimentally determined proportions (33% bast and 67% core fibres). The results are shown in Table 3.

Table 3. *Chemical Constitution of Hemp Plant*

Chemical components	***Bast* + *Core* (% ± relative error %)**	***Bast* (% ± relative error %)**	***Core* (% ± relative error %)**
Holocellulose	72.80 ± 0.06	86.40 ± 1.62	72.00 ± 0.22
Cellulose	53.25 ± 0.91	55.66 ± 0.53	47.34 ± 0.64
Total Lignin	21.80 ± 0.21	8.89 ± 0.22	25.35 ± 0.22
Extractives	2.00 ± 4.03	1.55 ± 2.32	1.79 ± 1.12
Ashes	2.59 ± 0.77	2.09 ± 2.04	2.53 ± 0.40

The results obtained for the different fractions are compatible with the literature values (Stevulova et al. 2014) or slightly lower with respect to the polysaccharides content, counterbalanced by the higher content of lignin (Gümüşkaya et al. 2007, Tutuş et al. 2014). The variability imposed by the plant growth conditions can justify the found discrepancies and, also, the similarities verified for plants grown in the Iberian Peninsula (Barberà et al. 2011). It should be noted the similarity with the chemical composition of the national *E. globulus:* Holocellulose - 72.0%; Extractives - 1.7%; Lignin - 22.1%; Ashes - 0.3% (Pinto et al. 2005); Lignin content: low - 20.5% and high - 23.0% (Cardoso et al. 2011),

particularly with regard to the determined lignin content (21.8%), which is atypical for a non-woody plant. This high content is determinant for any delignification process. However, the hemp plant ash amount is greater than eucalyptus wood, which is not a relevant fact for chemical pulping.

Raw Materials Cooking

The efficiency results of the kraft pulping processes performed to the whole hemp stalk and eucalyptus chips are presented in Table 4, which also exhibits the main unbleached pulp characteristics.

Table 4. *Cooking Process Results*

Unbleached pulp properties	**Hemp**	**Eucalyptus**
Pulp yield (%)	45.2	45.1
Uncooked pulp (%)	3.68	10.01
Kappa number	44.4	23.5
Intrinsic viscosity (mL/g)	991	1016
Degree of Polymerization	1489	1530

After carrying out the first hemp cooking, it was found that it was not possible to maintain the liquid-to-wood ratio of 5:1, possibly due to the structure and low density of the stems which have absorbed the entire cooking liquor, leaving no liquid phase for the circulation, essential factor for good impregnation and uniform heating of the cooking liquor. The lack of retting is another possible reason for this occurrence. Under these conditions it was chosen to increase the liquid-to-wood ratio to 7:1, and it was found that this volume of liquor was better suited to the cooking of this species. The cooking yields were similar for the two cooking essays, being 45.2% for hemp and 45.1% for eucalyptus. In previous studies carried out in Croatia and Spain the yield for hemp tow cooking with conventional kraft processes was 40% (Wong and Chiu 1995). Other authors from Poland reached total yields of 57.7% and 48.4% for whole stalks and woody-core fibres, respectively (Danielewicz and Surma-Ślusarska 2017), despite these values included pulp and fiberized uncooked knots. In the present study, the percentage of uncooked material (chips and knots) in the case of eucalyptus (10.1%) was higher than in the case of hemp, where the percentage of this material was residual (3.7%), probably due to the higher eucalyptus wood density.

Starting with two raw materials with identical lignin contents, it is noted that the extent of cooking was lower in the case of hemp because the kappa number determined in the unbleached hemp pulp (44.4) is about twice of the eucalyptus kappa number (23.5). This fact presupposes that the hemp delignification is harder. This difficulty in cooking hemp has already been observed in previous studies (Danielewicz and Surma-Ślusarska 2010). The selectivity of the cooking process is clearly superior for eucalyptus because the degree of polymerization obtained was higher and corresponds to a lower lignin content (DP = 1530, kappa number = 23.5) than in the case of hemp (DP = 1489, kappa number = 44.4). This feature shows that, with eucalyptus, a more efficient delignification occurred with a lower degradation of the cellulose chains and less liquid-to-wood ratio. The presence of a

very high amount of core fibres (67%) must explain the slow lignin removal and the difficult delignification of hemp fibres, as reported in other studies (Correia et al. 1998, Correia et al. 2001). Nevertheless, the DP obtained for the hemp pulp is typical for unbleached wood pulps (Tutuş et al. 2016).

Pulp Bleaching

The bleaching effect is shown in Figure 2.

Figure 2. *ECF Bleaching Results of Unbleached Pulps a) Evolution of ISO Brightness b) Evolution of Intrinsic Viscosity*

a)

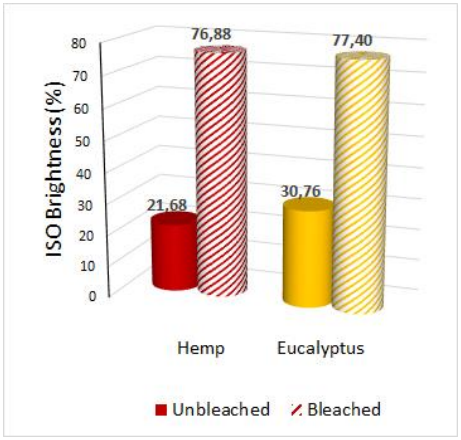

b)

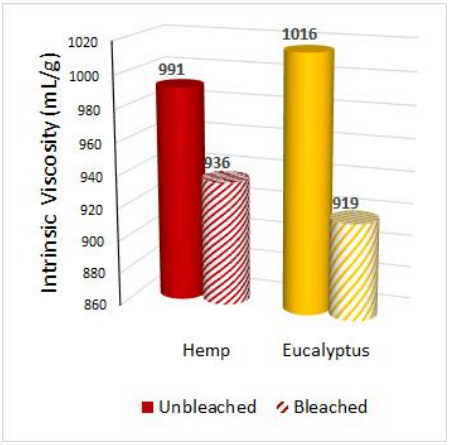

Hemp and eucalyptus bleached pulps show a similar ISO brightness as can be observed in Figure 2a. However, hemp pulp has a greater suitability for bleaching because it showed a higher increase in brightness (55.2%) compared to the increase attained for eucalyptus pulp (46.6%), since the reflectance of the unbleached pulp was initially lower. In United Kingdom, multi-step bleaching with chlorine dioxide was carried out for unbleached hemp tow pulp achieving a reflectance of about 24%, and final ISO brightness of 70% (Wong and Chiu 1995). In Poland, a hemp bleaching sequence with only two steps of chlorine dioxide and one alkaline extraction but preceded by an oxygen delignification, obtained a brightness of 88.6% (Danielewicz and Surma-Ślusarska 2017) revealing that an oxygen delignification stage before the first chlorine dioxide bleaching step really promotes a significant brightness improvement.

Pulps intrinsic viscosity variations are presented in Figure 2b and it is observed that the bleaching process led to a similar degradation of the polysaccharides (Smook 2016), being slightly higher in the case of eucalyptus (9.6%) than in the case of hemp (5.6%).

Properties of Paper Samples

As expected, due to the different fibre morphology, refining aptitude of the different pulps was quite distinct, as one can observe through Schopper-Riegler freeness values (ºSR) in Figure 3.

Figure 3. *Refining Curves - Pulps Beatability*

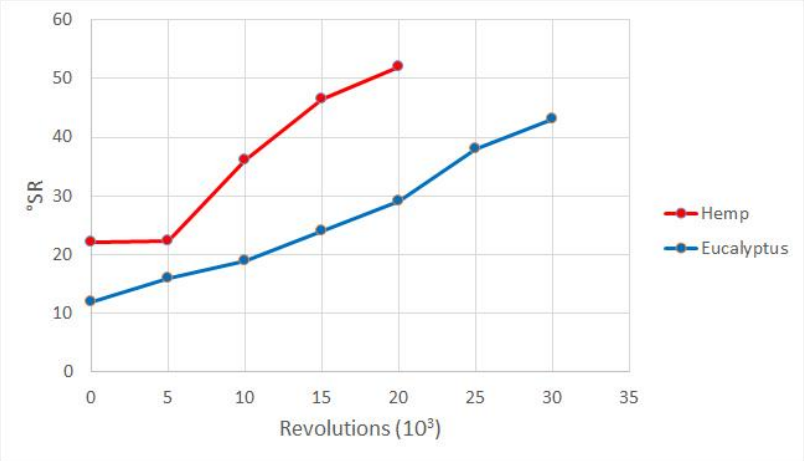

The beating process of unbleached hemp pulp presented satisfactory results compared with those obtained with the eucalyptus pulp (Figure 3), namely, easier refining, requiring a shorter residence time in the equipment to achieve the same beating degree, as already referred by other authors (Correia et al. 2003). This occurrence is possibly attributed to the high number of hemicelluloses present and to the smaller length of short core hemp fibres in comparison with eucalyptus fibres. This experimental observation finds some similarities in the research literature (Malachowska et al. 2015, Danielewicz and Surma-Ślusarska 2017). Nevertheless, the hemp pulp presented much worse drainage than eucalyptus pulp in the laboratory papermaking process, pointing to a higher fibrillation of the former, fact also documented in the literature (Danielewicz and Surma-Ślusarska 2017).

In this study, handsheets with diverse compositions exhibit distinctive results as shown in the following figures. Figure 4 presents the structural properties results – Bendtsen roughness and air permeability.

Figure 4. *Structural Properties vs. Fibrous Composition a) Bendtsen Roughness b) Bendtsen Air Permeability*

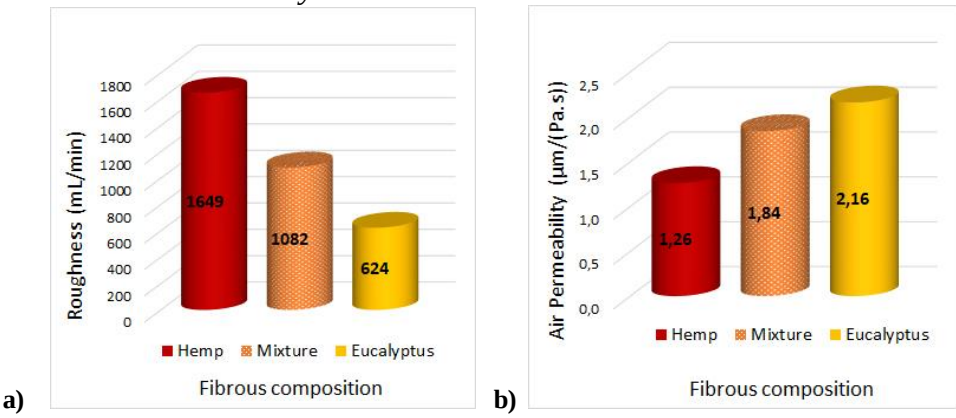

Analysing Figure 4a, one can observe that eucalyptus pulp handsheets reveal a roughness almost three times lesser than hemp handsheets. The mixture provided,

as expected, an intermediate value, fact attributed to the fibre's length and the homogeneity of this biometric parameter. Hemp pulp handsheets disclose a high roughness due to the strong difference between the lengths of bast fibres and short fibres (core). The bast fibres commit the paper formation and the ensuing smoothness, as one can perceive from the results presented by the paper obtained with the blend pulp. In Figure 4b, it is possible to check higher air permeability on eucalyptus pulp handsheets results. This property, such as roughness, varies also with the fibre bonding arrangement, being expected a higher permeability in the hemp pulp handsheets. This is not the case, probably due to the presence of high amount of short core fibres that fill the fibrous structure and reduce the pores that connect both sides of handsheets which were responsible for the air passage. The blend pulp handsheets have an intermediate air permeability, but nearer to the results of the eucalyptus pulp handsheets, considering the abundance of short core fibres of hemp with a length of about half of the average length of eucalyptus fibres (Foelkel and Zvinakevicius, 1980).

Paper strength is accountable for significant gains in runnability during printing and packaging processes therefore it is increasingly important to enhance mechanical paper properties. Among the strength properties, tearing resistance of hemp pulp handsheets outstands; tear index is superior to the others, as shown in Figure 5.

Figure 5. *Tear Index vs. Fibrous Composition*

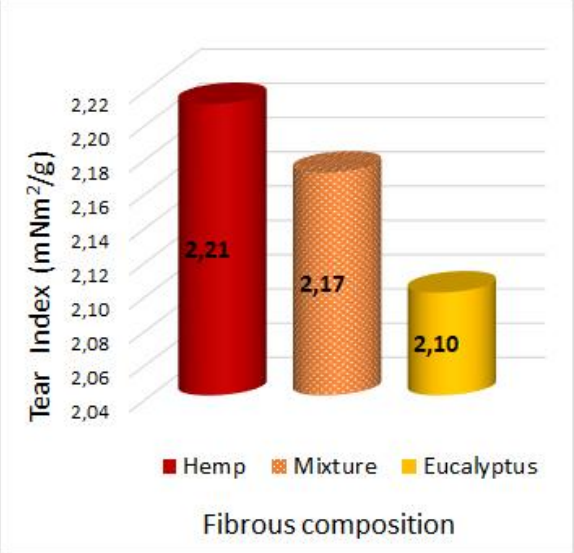

The influence of bast fibres length induces the highest tear index, and for the same reason, the blend pulp handsheets present an intermediate value of this property, slightly closer to the result obtained with the hemp pulp handsheets, revealing the importance of fibre length.

On the other hand, tensile strength of hemp handsheets (tensile index 42.4 N.m/g) is lower than the eucalyptus handsheets strength (tensile index 57.7 N.m/g) that is also mentioned in other studies about non-woody fibres (Karlsson et al. 2007, Danielewicz and Surma-Ślusarska 2017). The mixture handsheets showed

an intermediate tensile index (54.0 N.m/g), even though more approximate to the eucalyptus pulp value, which can possibly be explained by its fibrous constitution: a minor amount of bast fibres and a huger amount of eucalyptus and core small fibres (~17% of fibres with very high length and ~83% of fibres with an identical shorter length).

The relationship between handsheets' tear and tensile indexes is used as a parameter to assess the pulp and paper strength potential (Danielewicz and Surma-Ślusarska 2017). The hemp handsheets showed the highest tear index while eucalyptus handsheets revealed the highest tensile index, as shown in Figure 6.

The analysed mixture seems to exhibit an interesting behaviour, denoting a high tearing resistance while keeping a good tensile strength. This fact indicates that hemp plant fibres can be blended with eucalyptus fibres improving the mechanical performance of final paper, namely for packaging products.

Figure 6. *Tear-tensile Strength Relationship (Paper Potential)*

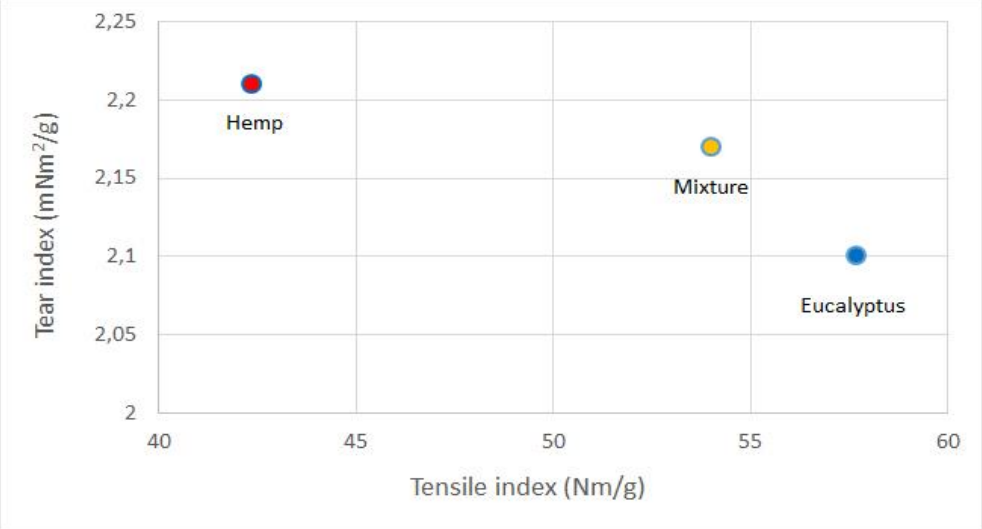

Conclusions

The whole stem of national industrial hemp presents cellulose content above 50% and high lignin content (similar of *Eucalyptus globulus* lignin content). Bast and core fibres have very different lengths, but similar widths.

In the kraft cooking process, hemp needed a larger liquid-to-wood ratio and presented greater difficulty of delignification than eucalyptus. Hemp and eucalyptus pulping have similar yields and produce pulps with identical cellulose polymerization degrees, but the kappa number of the unbleached pulp reveals that cooking is more extensive and selective in the case of eucalyptus.

Eucalyptus and hemp pulps, after being subjected to the same bleaching steps, exhibit identical ISO brightness, but hemp revealed a greater suitability for bleaching. Both bleached pulps viscosities are similar, nevertheless, hemp pulp reveals less degradation during the bleaching process.

When compared with a eucalyptus pulp, hemp pulp displays a better

beatability due to the presence of short core fibres and shows a higher tearing resistance justified by the presence of bast fibres.

In short, it seems that the hemp plant used integrally presents a good paper potential highlighting namely the bleachability, the beatability and the tearing resistance of unbleached pulps. The mixture of hemp and eucalyptus fibres (50:50) also reveals a good paper potential, exhibiting simultaneously very good tear and tensile strengths.

Acknowledgements

The authors wish to thank the laboratorial work developed by the Chemical and Biochemical Engineering Degree students under the authors' coordination, namely Afsar Ali, Luís Martins, Maria João Almeida, Rute Almeida and Soraia Henriques.

References

Aitken Y, Cadel F, Voillot C (1988) *Constituants fibreux des pâtes, papiers et cartons - pratique de l'analyse*. (Fibrous constituents of pulp, paper and cardboard - practice of analysis). Grenoble, France: Centre Technique du Papier et École Française de Papeterie et des Industries Graphiques.

Amaducci S, Scordia D, Liu FH, Zhang Q, Guo H, Testa G, Cosentino SL (2015) Key cultivation techniques for hemp in Europe and China. *Industrial Crops and Products* 68(Jun): 2-16.

Barberà L, Pèlach MA, Pérez I, Puig J, Mutjé P (2011) Upgrading of hemp core for papermaking purposes by means of organosolv process. *Industrial Crops and Products* 34(1): 865-872.

Bouloc P, Allegret S, Arnauld L (2013) *Hemp industrial production and uses*. Wollingford, UK: CABI Publishing, 328.

Cardoso GV, Foelkel CEB, Frizzo SMB, Rosa CAB, Assis TF, Oliveira P (2011) Efeito do teor de lignina da madeira de *Eucalyptus globulus* Labill no desempenho da polpação kraft. (Effect of lignin content of Eucalyptus globulus Labill wood on kraft pulping performance). *Ciência Florestal* 21(1): 133-147.

Correia F, Roy DN, Goel K (1998) Pulping of Canadian industrial hemp (*Cannabis sativa* L.): presents some findings of using non-wood sources. *Pulp and Paper Canada - Ontario*- 99(9): 39-41.

Correia F, Roy DN, Goel K (2001) Chemistry and delignification kinetics of Canadian industrial hemp (*Cannabis sativa* L.). *Journal of Wood Chemistry and Technology* 21(2): 97-111.

Correia F, Roy DN, Chute W (2003) Hemp chemical pulp: a reinforcing fibre for hardwood kraft pulps. *Pulp and Paper Canada –Ontario*- 104(5): 51-53.

Danielewicz D, Surma-Ślusarska B (2010) Processing of industrial hemp into papermaking pulps intended for bleaching. *Fibers & Textiles in Eastern Europe* 18(6): 110-115.

Danielewicz D, Surma-Ślusarska B (2017) Properties and fibre characterisation of bleached hemp, birch and pine pulps: a comparison. *Cellulose* 24(11): 5173-5186.

Danielewicz D, Surma-Ślusarska B, Kmiotek M, Dybka-Stępien K (2018) Susceptibility of selected non-wood fibrous raw materials for processing into unbleached and

bleached kraft pulps. *Cellulose Chemistry and Technology* 52(3-4): 283-289.

Danielewicz D, Surma-Ślusarska B (2019a) Bleached kraft pulps from blends of wood and hemp. Part I – demand for alkali, yield of pulps, their fractional composition and fibre properties. *Fibres & Textiles in Eastern Europe* 27(1): 112-117.

Danielewicz D, Surma-Ślusarska B (2019b) Bleached kraft pulps from blends of wood and hemp. Part II – structural, optical and strength properties of pulps. *Fibres & Textiles in Eastern Europe* 27(2): 111-116.

Foelkel CEB, Zvinakevicius C (1980) Hardwood pulping in Brazil. *Tappi* 63(3): 39-42.

Gümüşkaya E, Usta M, Balaban M (2007) Carbohydrate components and crystalline structure of organosolv hemp (*Cannabis sativa* L.) bast fibers pulp. *Bioresour Technology* 98(3): 491-497.

Hillig KW (2005) Genetic evidence for speciation in *Cannabis* (Cannabaceae). *Genetic Resources and Crop Evolution* 52(2): 161-180.

Johnson P (1999) Industrial hemp: a critical review of claimed potentials for *Cannabis sativa. Tappi* 82(12): 118-128.

Karlsson H, Beghello L, Nilsson L, Stolpe L (2007) Abaca as a reinforcement fibre for softwood pulp. *Tappi* 6(10): 25-32.

Lavoie JM, Beauchet R (2012) Biorefinery of *Cannabis sativa* using one- and two-step steam treatments for the production of high quality fibres. *Industrial Crops and Products* 37(1): 275-283.

Malachowska E, Przybysz P, Dubowik M, Kucner M, Buzala K (2015) Comparison of papermaking potential of wood and hemp cellulose pulps. *Annals of Warsaw University of Life Sciences - SGGW, Forestry and Wood Technology* 91: 134-137.

Pahkala K, Pahkala E, Syrjälä H (2008) Northern limits to fiber hemp production in Europe. *Journal of Industrial Hemp* 13(2): 104-116.

Pinto PC, Evtuguin DV, Pascoal Neto C (2005) Effect of structural features of wood biopolymers on hardwood pulping and bleaching performance. *Industrial and Engineering Chemistry Research* 44(26): 9777-9784.

Salentijna EMJ, Zhang Q, Amaducci S, Yang M, Trindade LM (2015) New developments in fiber hemp (*Cannabis sativa* L.) breeding. *Industrial Crops and Production* 68(Jun): 32-41.

Schluttenhofer C, Yuan L (2017) Challenges towards revitalizing hemp: a multifaceted crop. *Trends Plant Science* 22(11): 917-929.

Smook GA (2016) *Handbook for pulp and paper technologists*. 4th Edition. Atlanta, USA: Tappi Press.

Stevulova N, Cigasova J, Estokova A, Terpakova E, Geffert A, Kacik F, Singavszka E, Holub M (2014) Properties characterization of chemically modified hemp hurds. *Materials* 7(12): 8131-8150.

Tutuş A, Çiçekler M, Ozdemir F, Yilmaz U (2014) Evaluation of diospyros kaki grown in Kahra-manmaraş in pulp and paper production. In *Proceedings of the II National Mediterranean Forest and Environment Symposium*. Isparta, Turkey, October 22-24, 2014, 775-784.

Tutuş A, Karataş B, Çiçekler M (2016) Pulp and paper production from hemp by modified kraft method. In *Proceedings of the 1st IMSEC*. Adana, Turkey, October 26-28, 2016, 982-988.

Wong A, Chiu C (1995) Pulping and bleaching of hemp (*Cannabis sativa*). In *Proceedings of the Tappi Pulping Conference*. Chicago, USA, October 1-5, 1995, 471-476.

Athens Journal of Sciences 2020, 7(1):29-42
https://doi.org/10.30958/ajs.7-1-3

Mathematical Analysis of the Implication of the Proposed Rise in the Retirement Age on the Unemployment Situation in Nigeria

By Abayomi Ayoade[*], Rotimi Folaranmi[±] & Tolulope Latunde[‡]

The population of Nigeria as of today stands at about 200,000,000. The economically active or working population (15-64 years) increased from 111.1 million in 2017 to 115.5 million in 2018. The unemployment rate accordingly, rose from 18.8% in 2017 to 23.1% in 2018. The situation has aggravated poverty and brought about untold hardship particularly for the unemployed. Currently, there is intense debate regarding the adjustment in the statutory age of retirement in Nigeria. To that end, a deterministic compartmental mathematical model is designed to study the implication of the proposed increase in the national statutory age of retirement on the national output and the trend of unemployment in Nigeria. The mathematical interpretation of the compartments of the model leads to the corresponding first-order ordinary differential equations. The resulting equations are proved to satisfy the basic features of a good mathematical model. The unemployment-free equilibrium is derived and the stability analysis is performed via stability theory of nonlinear differential equations. Numerical simulation is conducted to validate the analytical results. Results from the simulation show that increasing the national statutory age of retirement will limit the rate at which individuals are moving from the unemployed state to the employed state but widen the rate at which individuals are joining and remaining in the unemployed state.

Keywords: *Poverty, Retirement, Model, Unemployment rate, Simulation*

Introduction

Unemployment is a major problem in Nigeria and other Third World that have a similar economic structure with Nigeria. Unemployment is an economic and social disorder which arises as a result of the imbalance between supply and demand in the labour market and sometimes aggravated by the population's growth. The unemployed class of a population can be said to be the proportion of the population who are able and desire to work but, as a result of inadequate demand, are unable to secure jobs. Usually, unemployment is a terrible social condition since a proportion of the population battles to endure the least welfare and consumption level. The labour force of a country is the sum of employed and unemployed individuals in the country. The age bracket for labour force varies from one country to another and from one profession to another profession. For

[*]Lecturer II, Department of Mathematics, University of Lagos, Nigeria.
[±]Lecturer II, Department of Mathematical and Computing Sciences, KolaDaisi University, Nigeria.
[‡]Lecturer II, Department of Mathematics, Federal University Oye-Ekiti, Nigeria.

example, in Nigeria, the statutory retirement age for professors and judges is 70 years while it is 65 years for other academic staff in tertiary institutions. The statutory retirement age drops to 60 years for teachers in both secondary and elementary schools. However, the labour force in Nigeria generally encompasses all individuals aged 15-64 years who desire to work irrespective of whether they secure jobs or not.

The population of Nigeria currently stands at about 200,000,000 with a growth rate of 2.62% in 2018. The economically active population is more than 50% of the total population with the figure of 115,500,000 of which 26,680,500 are unemployed as at December 2018 (National Bureau of Statistics-NBS 2018). The situation has aggravated poverty and made life difficult in Nigeria. The rapid growth rate of the population has also exacerbated the unemployment rate. Currently, there is intense debate regarding the adjustment in the statutory age of retirement. Some individuals and organisations have been calling for rising in the statutory age of retirement which some state governments in Nigeria have yielded to. For instance, the Ondo state government of Nigeria has announced an increase in the statutory age of retirement for workers of her tertiary institutions in May 2019. The State government approved 70 years for professors as the new retirement age and 65 years for other staff of her tertiary institutions. The unemployment rate has been rising in Nigeria over the years. Table 1 shows the trend of the unemployment rate and quarterly change in 2015-2018 in Nigeria.

Table 1. *Unemployment Rate and Quarterly Change in 2015-2018*

Period	**Unemployment rate (%)**	**Rate of quarterly change (%)**
2015q1	7.54	
q2	8.19	0.65
q3	9.9	1.71
q4	10.44	0.54
2016q1	12.09	1.64
q2	13.32	1.24
q3	13.88	0.56
q4	14.23	0.35
2017q1	14.44	0.21
q2	16.18	1.74
q3	18.8	2.62
q4	20.42	1.62
2018q1	21.83	1.41
q2	22.73	0.92
q3	23.13	0.4

Source: NBS 2018.

The aim of this paper is to use mathematical modelling method to investigate the implication of the proposed increase in the national statutory age of retirement on the national production and the current trend of unemployment in Nigeria.

Literature Review

X-raying the available literature on the subject, we start from 2011 when Misra and Singh (2011) designed a model of unemployment based on the previous work of Nikolopoulos and Tzanetis (2003). Nikolopoulos and Tzanetis (2003) developed a model taking into consideration the allocation of houses for a homeless population induced by a natural disaster, described in terms of a system of nonlinear ordinary differential equations with three variables –employed individuals, unemployed individuals, and temporary workers. Misra and Singh (2011) analysed the equilibria of their proposed model, applying the stability theory, and conducted some numerical simulations, revealing that the unemployment struggle might need urgent interventions: they predicted that the unemployment rate might rise continuously and, if the peak was reached then it would be difficult to overcome in future.

Misra and Singh (2013) also came out with an empirical work when they substituted the temporarily employed variable with newly created vacancies incorporating a delayed feature in their previous study of Misra and Singh (2011). Another model of unemployment was also formulated by Sirghi et al. (2014) based on the system of differential equations with distributed time delay. Besides, they discovered that the unemployment level was signal to the employers to hire labourers at low wages. The separation of the available vacancies into government and current created vacancies was a major modification to the earlier works of Misra and Singh (2011) and Misra and Singh (2013) by Harding and Neamtu (2018). Harding and Neamtu adopted the idea of Misra and Singh (2011) and Misra and Singh (2013), modifying the earlier efforts by formulating an unemployment model in which job searches are open to both migrant and native workers.

In the same way, by taking into account the previously mentioned works, Munoli and Gani (2016) attempted to examine an optimal control policy for unemployment considering two possible interventions: government policies, designed to provide jobs directly to unemployed individuals, and government policies, designed to create new vacancies. The situation in Munoli and Gani (2016) of the labour market was governed by three first order ordinary differential equations, pointing to variation in vacancies available and unemployed/employed, quite similar to Misra and Singh (2013). Inspired by the work of Munoli and Gani (2016), Galindro and Torres (2018) proposed an unemployment model and applied optimal control to investigate the appropriate policies for avoiding unemployment in Portugal. Kazeem, Alimi and Ibrahim (2018) designed an unemployment model and derived a threshold quantity for the control of unemployment. They discovered that the unemployment solution in Nigeria was a function of self-employment as academic certificates cannot bring food on the table. El Fadily and Kaddar (2019) also developed a model to monitor labour force evolution and discovered the phenomenon of co-existence of both active unemployed and employed populations. They explained the phenomenon of co-existence of the two populations in terms of the fact that job seekers occur relatively quickly because of population growth.

A good number of factors can shape unemployment situation apart from statutory age of retirement. For example, Aminu (2019) opined that there was mismatch between the university training and the needs of the labour market which gave birth to education-job mismatch in Nigeria. Also, Teixeira et al. (2020) argued that Brazilian workers were influenced by the government programmes as to the length of stay in the job which might have the tendency of enhancing the low incentive for companies to invest in human capital, encouraging turn over in the Brazilian labour market and generating the average low productivity of the national workers. Unemployment has negative impacts on the general well-being and the economy of a nation. The links between unemployment, poverty and economic growth in Nigeria was investigated by Adelowokan et al. (2019). The authors discovered that while unemployment had a positive and significant relationship with poverty at the conventional level, it had a negative and important relationship with growth. The result of the study of Adelowokan and co researchers (2019) was corroborated by the outcome of the study conducted by Yasin and Gachunga (2019) where a negative long run relationship was established between unemployment and economic growth in Kenya. In an attempt to substantiate the negative impact of unemployment on societal stability, Amin (2019) formulated a mathematical model of crime and unemployment to conduct a study on the relationship between crime and unemployment. The researcher established a rapid increase in the volume of crime as the unemployment rises. While the mathematical studies of unemployment are exhaustive in the literature, we are not aware of the one that is directed to the implication of an increase in the age of retirement with reference to the unemployment situation in Nigeria.

Methodology

The global rise in unemployment rate due to the enormous upsurge in world population prompted Munoli and Gani (2016) to formulate a mathematical model that captured an unemployment environment with an optimal control strategy for the deterministic unemployment model. The model is made up of three first-order ordinary differential equations, with the employed *(E),* unemployed *(U)* and the vacancies *(V)* as the state variables:

$$\left.\begin{aligned}
\frac{dU(t)}{dt} &= \pi - \kappa U(t)V(t) - \alpha_1 U(t) + \gamma E(t),\\
\frac{dE(t)}{dt} &= \kappa U(t)V(t) - \alpha_2 \mathrm{E}(t) - \gamma E(t),\\
\frac{dV(t)}{dt} &= \alpha_2 \mathrm{E}(t) + \gamma E(t) - \delta \mathrm{V}(t) + \phi
\end{aligned}\right\} \qquad (1)$$

The interpretation for the state variables and parameters of Eq. (1) is presented in Table 2.

Table 2. *Variables/Parameters Description*

Variables/Parameters	Meaning
$U(t)$	Population of the unemployed at time t
$E(t)$	Population of the employed at time t
$V(t)$	Available vacancies at time t
π	Recruitment rate into $U(t)$
κ	Rate at which unemployed individuals are becoming employed
α_1	Rate of migration and death of unemployed individuals
α_2	Rate of retirement and death of employed individuals
γ	Rate at which individuals are fired from their present job
ϕ	Rate at which new vacancies are created
δ	Rate of reduction in vacancies due to recession

Source: Munoli and Gani (2016).

The necessary and sufficient conditions for the attainment of optimal control of the proposed unemployment problem with the efficient use of implemented strategies to create employment to the unemployed individuals and to provide new vacancies were derived and analysed by Munoli and Gani (2016). However, the implication of the adjustment in the statutory age of retirement in creating employment for the unemployed and in generating new vacancies was not considered by the authors. It is against this backdrop that the present study attempts to extend the model to investigate the implication of the proposed rise in the statutory age of retirement on the current unemployment situation in Nigeria. As unemployment and underemployment coexist simultaneously in Nigeria, the possibility of the increase in the population of the unemployed due to the influx of those who leave their current employment as a result of lack of job satisfaction without immediate hope of securing the satisfactory employment and the newly created vacancies due to the action is considered. Also, following the idea of Galindro and Torres (2018), the rate at which employment is being created is considered. If the rate at which individuals leave their current jobs as a result of lack of job satisfaction is β and the rate at which the employment is created is ω then the system of Eq. (1) becomes

$$\left.\begin{aligned}
\frac{dU(t)}{dt} &= \pi - \kappa U(t)V(t) - \alpha_1 U(t) + \gamma E(t) + \beta E(\mathrm{t}),\\
\frac{dE(t)}{dt} &= \kappa U(t)V(t) - \alpha_2 \mathrm{E}(t) - \gamma E(t) - \beta E(\mathrm{t}) + \omega,\\
\frac{dV(t)}{dt} &= \alpha_2 \mathrm{E}(t) + \gamma E(t) + \beta E(\mathrm{t}) - \delta \mathrm{V(t)} + \phi
\end{aligned}\right\} \qquad (2)$$

The variables and parameters interpretations for Eq. (2) together with their values and sources are presented in Table 3.

Table 3. *Variables/Parameters Description, their Values and Sources*

Variables/Parameters	Meaning	Values	Sources
$U(t)$	As in Table 2	10000	Munoli and Gani (2016)
$E(t)$	As in Table 2	1000	Munoli and Gani (2016)
$V(t)$	As in Table 2	100	Munoli and Gani (2016)
π	As in Table 2	5000	Munoli and Gani (2016)
κ	As in Table 2	0.000009	Munoli and Gani (2016)
α_1	As in Table 2	0.04	Munoli and Gani (2016)
α_2	As in Table 2	0.05	Munoli and Gani (2016)
γ	As in Table 2	0.001	Munoli and Gani (2016)
ϕ	As in Table 2	0.007	Munoli and Gani (2016)
δ	As in Table 2	0.005	Assumed
β	Rate at which people leave their jobs due to job dissatisfaction	0.0001	Assumed
ω	Rate of employment creation	0.0002	Assumed

Theorem 1: The solutions of the system of Eq. (2) exist and are unique in $\Re^3$. Suppose the system of Eq. (2) is represented as

$$f_1 = \pi - \kappa U(t)V(t) - \alpha_1 U(t) + \gamma E(t) + \beta E(t) \quad (3)$$

$$f_2 = \kappa U(t)V(t) - \alpha_2 \mathrm{E}(t) - \gamma E(t) - \beta E(t) + \omega \quad (4)$$

$$f_3 = \alpha_2 \mathrm{E}(t) + \gamma E(t) + \beta E(t) - \delta V(t) + \phi \quad (5)$$

then, let D denotes the region

$$|\mathrm{t}-\mathrm{t}_0| \le \mathrm{a}, \|\mathrm{x}-\mathrm{x}_0\| \le \mathrm{b}, \mathrm{x} = (x_1, x_2, \cdots, x_n), \mathrm{x}_0 = (x_{10}, x_{20}, \cdots, x_{n0}),$$

and suppose that $f(t,x)$ satisfies the Lipschitz condition

$$\|(\mathrm{t}, \mathrm{x}_1) - \mathrm{f}(\mathrm{t}, \mathrm{x}_2)\| \le \mathrm{k}\,\|\mathrm{x}_1 - \mathrm{x}_2\|.$$

Whenever the pairs (t, x_1) and (t, x_2) belong to $D^{|}$, where *k* is a positive constant, then, there is a constant $\delta > 0$ such that there exists a unique continuous vector solution *x (t)* of the system in the interval $t - t_0 \le \delta$. It is important to note that the condition is satisfied by requirement that $\frac{\partial f_1}{\partial x_j}, i = 1, 2, \ldots$ be continuous and bounded in $D^{|}$

Proof:
We now return to our model Eq. (3) – Eq. (5). We are interested in the region $0 \le \alpha \le \Re$.

We look for a bounded solution in this region and whose partial derivatives satisfy $\delta \le \alpha \le 0$, where α and δ are positive constants.

Suppose $D^{|}$ denotes the region $0 \le \alpha \le \Re$ then, Eq. (3) – Eq. (5) have a unique solution if it is established that $\frac{\partial f_1}{\partial x_j}, i, j = 1, 2, 3$ are continuous and bounded in $D^{|}$.

Using Eq. (3), we have the partial derivatives:
$$\left|\frac{\partial f_1}{\partial U}\right| = \left|-\kappa V - \alpha_1\right| < \infty, \left|\frac{\partial f_1}{\partial E}\right| = \left|\gamma + \beta\right| < \infty, \left|\frac{\partial f_1}{\partial V}\right| = \left|-\kappa U\right| < \infty$$

These partial derivatives exist, continuous and are bounded. For Eq. (4), we have:
$$\left|\frac{\partial f_2}{\partial U}\right| = \left|\kappa V\right| < \infty, \left|\frac{\partial f_2}{\partial E}\right| = \left|-\alpha_2 - \gamma - \beta\right| < \infty, \left|\frac{\partial f_2}{\partial V}\right| = \left|\kappa U\right| < \infty$$

and
$$\left|\frac{\partial f_3}{\partial U}\right| = 0 < \infty, \left|\frac{\partial f_3}{\partial E}\right| = \left|\alpha_2 + \gamma + \beta\right| < \infty, \left|\frac{\partial f_3}{\partial V}\right| = \left|-\delta\right| < \infty$$

Since all the partial derivatives exist and are finite (bounded and defined), the solutions of the system of equations exist and are unique in $\Re^3$. This completes the proof.

Theorem 2: The region of attraction for the human compartments of the model represented by Eq. (3) and Eq. (4) is given by $\Gamma = \left\{(U, E) : 0 \le U + E \le \frac{\pi + \omega}{m}\right\}$,

where $m = \min(\alpha_1, \alpha_2)$ and it attracts every solution in the interior of the positive octant.

Proof:
Eq. (3) + Eq. (4) $\Rightarrow$

$$\frac{d}{dt}\left(U(t)+E(t)\right)=\pi-\alpha_1 U(t)-\alpha_2 E(t)+\omega \Rightarrow$$

$$\frac{d}{dt}\left(U(t)+E(t)\right)\leq \pi+\omega-m\left(U(t)+E(t)\right)$$

where $m=\min\left(\alpha_1,\alpha_2\right)$.

By taking limit supremum,

$$\limsup_{t\to 0}\left(U(t)+E(t)\right)\leq \frac{\pi+\omega}{m}$$

This completes the proof.

Theorem 3: The solution of the vacancy compartment *V(t)* is also positive since every initial condition to the variable is always nonnegative.

Proof:

$$\frac{dV}{dt}=\alpha_2 E(t)+\gamma \mathrm{E(t)}+\beta \mathrm{E(t)}-\delta \mathrm{V(t)}+\phi \Rightarrow$$

$$\frac{dV}{dt}\geq -\delta V(t) \Rightarrow$$

$$\frac{dV}{V(t)}\geq -\delta dt \Rightarrow$$

$$\int \frac{dV}{V}\geq -\int \delta dt$$

Using the separation of variable method and applying the initial condition, we obtain

$$\mathrm{V}(t)\geq V_0 e^{-\delta t}\geq 0 \ . \qquad (6)$$

Since e^n is always positive for every real value of *n* then, the solution of *V(t)* is always positive.

This completes the proof.

Model Analysis

Equilibria

The model system (2) has an unemployment-free equilibrium, F_0 which is derived by reducing all the unemployment terms and the RHS of the model to zero. The result is obtained as:

$$F_0 = \left(\mathrm{U}^0, \mathrm{E}^0, V^0\right) = \left(0, \frac{\omega}{\alpha_2 + \gamma + \beta}, \frac{\phi + \omega}{\delta}\right) \tag{7}$$

Stability Analysis of the Unemployment-Free Equilibrium, F_0

Theorem 4: The unemployment-free equilibrium of the model is locally asymptotically stable if all the eigenvalues of the variational matrix of the system (2) are negative.

Proof: The variational matrix of the system (2) at the unemployment-free equilibrium is obtained as

$$J\left(F_0\right) = \begin{pmatrix} \frac{-\kappa}{\delta}\left(\phi + \omega\right) - \alpha_1 & \left(\beta + \gamma\right) & 0 \\ \frac{\kappa}{\delta}\left(\phi + \omega\right) + \alpha_1 & -\left(\alpha_2 + \beta + \gamma\right) & 0 \\ 0 & \left(\alpha_2 + \beta + \gamma\right) & -\delta \end{pmatrix} \tag{8}$$

Eq. (8) has the characteristic equation

$$p_0\lambda^3 + p_1\lambda^2 + p_2\lambda + p_3 = 0 \tag{9}$$

where,

$$\left.\begin{aligned} p_0 &= 1 \\ p_1 &= \frac{\kappa}{\delta}\left(\phi + \omega\right) + \alpha_1 + \alpha_2 + \beta + \gamma + \delta \\ p_2 &= \frac{\kappa}{\delta}\left(\phi + \omega\right)\left(\alpha_2 + \delta\right) + \alpha_1\delta + \left(\alpha_1 + \delta\right)\left(\alpha_2 + \beta + \gamma\right) \\ p_3 &= \kappa\alpha_2\left(\phi + \omega\right) + \alpha_1\delta\left(\alpha_2 + \beta + \gamma\right) \end{aligned}\right\} \tag{10}$$

Using Routh-Hurtwitz stability criteria as in Galindro and Torres (2018), the unemployment free equilibrium of the model is locally asymptotically stable if the conditions $p_1 > 0, p_3 > 0$ and $p_1 p_2 - p_3 > 0$ are satisfied in Eq. (9). This is the necessary and sufficient condition for all the roots of Eq. (9) to have negative real parts which imply stable equilibrium. Obviously, $p_1 > 0$ and $p_3 > 0$ are satisfied

since all the model parameters are non-negative. Therefore, the unemployment free equilibrium of the model system (2) is stable if $p_1 p_2 - p_3 > 0$.

Results and Discussion

Unemployment-free equilibrium is the equilibrium point in the absence of unemployment. It is a stage when a society attains full employment. At this point, it is assumed that nobody is unemployed in society. In reality, full employment is only possible in theory but not realistic in practice as some individuals may decide to be voluntarily unemployed regardless of the presence of employment. Even in a very buoyant economy like that of the United Arab Emirate and Qatar, the unemployment rate is still greater than zero, 1.72 and 0.10 respectively (NBS 2018). The stability of the unemployment-free equilibrium implies that the unemployment rate is kept at bay while the instability of the unemployment-free equilibrium implies that the unemployment rate has gone out of hand.

The first two conditions of the Routh-Hurwitz stability criteria have already been met. In order to draw a conclusion as regards the stability or otherwise of the model, there is a need to verify the third condition. To come about this, the values in Table 3 are taken as the base for each parameter to evaluate the initial value of $p_1 p_2 - p_3$ which is given in S/No 1 of Table 4. The values of α_2, κ and ϕ are then varied to investigate the effect of the adjustment in the statutory age of retirement on the stability nature of the model and the result is presented in Table 4. The result in Table 4 is then supported graphically in Figure 1.

Table 4. *Stability Result of the Model*

S/No	α_1	α_2	β	κ	ϕ	ω	γ	δ	$p_1 p_2 - p_3$	Remark
1	0.04	0.05	0.0001	0.000009	0.007	0.0002	0.001	0.005	0.000	Unstable
2	0.04	0.06	0.0001	0.00001	0.008	0.0002	0.001	0.005	0.000	Unstable
3	0.04	0.07	0.0001	0.00002	0.009	0.0002	0.001	0.005	0.000	Unstable
4	0.04	0.08	0.0001	0.00003	0.01	0.0002	0.001	0.005	0.000	Unstable
5	0.04	0.09	0.0001	0.00004	0.02	0.0002	0.001	0.005	0.001	Stable
6	0.04	0.1	0.0001	0.00005	0.03	0.0002	0.001	0.005	0.001	Stable
7	0.04	0.2	0.004	0.00006	0.04	0.0002	0.001	0.005	0.002	Stable
8	0.04	0.3	0.005	0.00007	0.05	0.0002	0.001	0.005	0.005	Stable
9	0.04	0.04	0.005	0.000008	0.006	0.0002	0.001	0.005	0.000	Unstable
10	0.04	0.03	0.005	0.000007	0.005	0.0002	0.001	0.005	0.000	Unstable
11	0.04	0.02	0.005	0.000006	0.004	0.0002	0.001	0.005	0.000	Unstable
12	0.04	0.01	0.005	0.000005	0.003	0.0003	0.001	0.005	0.000	Unstable

Figure 1. *Possible Employment Situation in Nigeria in a Century*

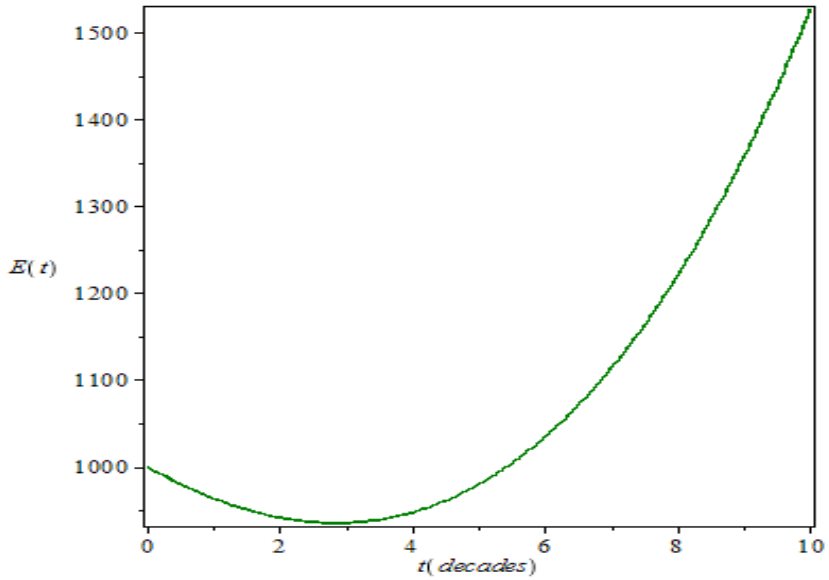

The current statutory age of retirement in Nigeria is 60 years. Generally, an increase in the rate of retirement which may be facilitated through a reduction in the statutory age of retirement will raise the rates at which new vacancies are being created and at the same time, the rates at which the unemployed individuals are becoming employed. On the other hand, a decrease in the rate of retirement which may be brought about by an increase in the statutory age of retirement will limit the rates at which new vacancies are being created and the rate at which the unemployed people are becoming employed. This is corroborated in Table 4. As an increase in the retirement rate (α_2) is accompanied by the simultaneous increase in the vacancies (ϕ) and the movement rate from the unemployed class to the employed class (κ), the model is at start, unstable (S/No 2 – S/No 4 in Table 4) but finally reaches the stable region (S/No 5 – S/No 8 in Table 4). On the other hand, as a decrease in the retirement rate is followed by the corresponding decrease in the vacancies and the movement rate from the unemployed class to the employed class, the model continues to be unstable (S/No 9 – S/No 12 in Table 4).

The implication of the result is that the current proposal of the increase in the statutory age of retirement in Nigeria is not only suicide but evil to the future of the younger and coming generations. As a good number of the working class in Nigeria are engaging in paid employment, increasing the statutory age of retirement will exacerbate the already worsen unemployment situation in the country. Besides, increasing the national statutory age of retirement above 60 years may have a decreasing effect on the national output as a good number of individuals above 60 years may have past their prime.

In Figure 1, if the current statutory age of retirement is increased then in 30 years time, more individuals will join and remain in the unemployed state but if the current statutory age of retirement is reduced then in 40 years time, more and more unemployed individuals will begin and continue to move to the employed

state. Therefore, since the rates of increase in both labour force and unemployment is outrageous in Nigeria, encouraging the working class to go on voluntary retirement either by cash reward or by allowing them to replace themselves with an unemployed individual of their choice will reduce the rate of unemployment, put employment situation in the stable region (i.e. S/No 5 – S/No 8 in Table 4) and ensure better future for the younger and coming generations.

Conclusions

A nonlinear mathematical model for unemployment proposed in Munoli and Gani (2016) was extended to study the implication of the proposed rise in the statutory age of retirement on the unemployment situation in Nigeria by incorporating the rate at which the employment was being created and the tendency of upsurge in the population of the unemployed due to the influx of individuals who left their current job as a result of lack of job satisfaction. The solutions of the model were proved to exist, unique and positive. Equilibrium analysis was conducted and the unemployment-free equilibrium was obtained. Stability analysis of the unemployment-free equilibrium was also performed and the numerical simulation was carried out to verify the analytical results. The results of the simulation were finally discussed.

References

Adelowokan OA, Maku OE, Babasanya AO, Adesoye AB (2019) Unemployment, poverty and economic growth in Nigeria. *Journal of Economics and Management.* 35(1): 4-11.

Amin R (2019) Mathematical model of crime and unemployment. *International Journal of Engineering Research & Technology* 8(9): 33-41.

Aminu A (2019) Characterising graduate unemployment in Nigeria as education-job mismatch problem. *African Journal of Economics Review* 7(2): 113-130.

El Fadily S, Kaddar A (2019) Modelling and mathematical analysis of labour force evolution. *Hindawi Modelling and Simulation in Engineering.* DOI: http://doi.org/ 10.1155/2019/2562468

Galindro A, Torres DFM (2018) A simple mathematical model for unemployment: a case study in Portugal with optimal control. *Statistics, Optimization and Information Computing* 6(Apr): 116-129.

Harding L, Neamtu M (2018) A dynamic model of unemployment with migration and delayed policy intervention. *Computational Economics* 51(3): 427-462. DOI: 10.1007/s10614-016-9610-3.

Kazeem AB, Alimi SA, Ibrahim MO (2018) Threshold parameter for the control of unemployment in the society: mathematical model and analysis. *Journal of Applied Mathematics and Physics* 6 (Dec): 2563-2578. DOI: 10.4236/jamp.2018.612214.

Misra AK, Singh AK (2011) A mathematical model for unemployment. *Nonlinear Analysis Real World Application* 12(1): 128-136.

Misra AK, Singh AK (2013) A delay mathematical model for the control of unemployment. *Differential Equation Dynamical System* 21(3): 291-307.

Munoli SB, Gani S (2016) Optimal control analysis of a mathematical model for unemployment. *Optimal Control Application Methods* 37(Nov): 798-806.

National Bureau of Statistics-NBS (2018) *Labour force statistics-volume1: unemployment and underemployment report*. Retrieved from: https://nigerianstat.gov.ng/download/694. [Accessed 3 January 2019].

Nikolopoulos CV, Tzanetis DE (2003) A model for housing allocation of a homeless population due to natural disaster. *Nonlinear Analysis* 4(Oct): 561-579.

Sirghi N, Neamtu M, Deac DS (2014) A dynamic model for unemployment control with distributed delay. *Mathematical Methods in Finance and Business Administration* 12 (Apr): 42-48.

Teixeira GS, Neto GB, Leivas PHS (2020) Evidence on rule manipulation and moral hazard in Brazilian unemployment insurance program. *International Journal of Social Science Studies* 8(1): 67-78.

Yasin K, Gachunga MJ (2019) An analysis of the impact of unemployment on economic growth in Kenya. *International Journal of Business Marketing and Management* 4(4): 52-57.

Athens Journal of Sciences 2020, 7(1): 43-66
https://doi.org/10.30958/ajs.7-1-4

A Practical Approach of Different Programming Techniques to Implement a Real-time Application using Django

By Sebastian Stigler[*] & Marina Burdack[‡]

Real-time web-applications surround our daily life. The most popular are shopping platforms like Amazon or Zalando. Behind these websites huge and complex shop-systems are typically used. These systems manage and handle thousands of parallel synchronous and asynchronous tasks like user interactions, user authentications, communication with an ERP system (enterprise resource planning), or the handling of the website visualization in the background. Through the independence of the computer system and the portability on other devices, like touch panels or mobile phones the web-technology is also used for industry 4.0 applications. The applications can be e. g. predictive maintenance dashboards or monitoring dashboards for the production line. The key task for these dashboards are the visualization and analyzing of a huge amount of data in real-time. For both scenarios, the data have to be preprocessed continuously in different steps. In summary, the industry 4.0 application has to manage a different kind of tasks compared to a typical webshop. These tasks contain for example big data preprocessing tasks, which are mostly CPU bound, in contrast to the typically I/O bound task of a webshop (e.g. database access). The main problem with web application frameworks is that they are not designed to execute a lot of CPU bound tasks and handle webrequests at the same time. The purpose of this paper is to compare two different programming techniques for the work with CPU bound tasks in a real-time web application for the use in industry 4.0 without the use of third-part software like Spark. The research employed two approaches: on the one hand multiprocessing and on the other hand task queues. In this work, two kinds of web-applications on the base of python's web framework Django are implemented. The first application uses multiprocessing and the second application uses the Celery task queue to organize different tasks. The general building blocks are the sensor data streaming via MQTT and the data transformation in various steps. The result of this transformation can be used to visualize the data in real-time charts for example. The implemented web-applications are evaluated by the following criteria:

- *Performance while working with a huge amount of streaming data.*
- *Possibilities to optimize the load distribution and avoid overloading.*
- *Possibilities to scale up and down hardware.*

Keywords: *Django, Machine Learning, Multithreading, Real-Time-Application, Task Queue.*

[*]Research Fellow, Aalen University of Applied Sciences, Germany.
[‡]Research Fellow, Aalen University of Applied Sciences, Germany.

Introduction

Real time web applications surround our daily life. Different web applications can be found in different areas like the web shops or google, but also in different areas like the industry or the medical sector. Both sectors work with real time streaming data. In the industry 4.0 often monitoring dashboard are built, which analyze sensor data from machines for example for predictive maintenance or for quality prediction (Burdack and Rössle 2019, Rössle and Kübler, 2017). In the medical sector, web applications are used for the tracking of medicine intakes for example (Vinjumur et al. 2010).

But all these different applications consist of more than one component. All these applications need a database or a data storage, their own business logics, user authentication and so on. But the highest influence on the performance of the web applications has the streaming data. In industry 4.0 settings there is a big amount of sensor data, which need to be processed and stored in the application for further analytics or machine learning purpose. All these approaches follow the standard CRISP model (Wirth 2000), where a central point is the data preparation or in the field of machine learning it is called data preprocessing. These approaches are the typical working areas of data scientists.

The most popular programming language in Data Science for data analysis and web development is ***python*** (Kaggle, et al. 2018, Python Software Foundation and JetBrains 2018). According to Python Software Foundation and JetBrains (2018) ***Django*** and ***Flask*** are the most popular web frameworks in python.

But the program language and a web framework are not enough for a real-time application. Especially for working with a big amount of data, there is often third party software[1] like Spark (Meng et al. 2016), Hadoop (Borthakur et al. 2011) or AirFlow (Kotliar et al. 2018) needed to scale the application, and thus to schedule the working tasks.

Nevertheless, all these tools only work with good performance, if they are configured by data scientists with long experience in using them. But these experiences are often not available in young data scientist teams or the effort for the implementation for a small project is too high.

For this research work, a Django application was developed, which allows to configure and run different preprocessing tasks efficiently. In addition, our implementation allows to configure and run machine learning tasks too, without any changes. Only the different machine learning tasks have to be implemented and registered in the application database. Through the strict definition of tasks, different data processing pipelines can be modeled with this approach beginning with the configuration of the data source (MQTT, streaming database ...) and ending with the visualization or presentation of the results. All can be done in one application.

This article focuses on the most important part in the machine learning pipeline: the preprocessing of data. The findings and results of this approach are

[1]Which are not written in python.

used in the implementation of the whole framework for machine learning in Burdack and Rössle (2019). This leads to the following research questions:

- Is it possible to implement the preprocessing part of the machine learning pipeline in an industry 4.0 real-time web application, without the use of (non python) third party software in python?
- How can you scale the application in an easy way, if the amount of incoming data increases significantly?

Literature Review

In literature different approaches and software solutions exist to develop software applications, which work efficient and are scalable.

The most popular software for scaling software applications, especially in the field of big data and machine learning are Apache Spark (Meng et al. 2016) (https://spark.apache.org/), and Hadoop (Borthakur et al. 2011).

"*Apache Spark is a popular open-source platform for large-scale data processing that is well-suited for iterative machine learning tasks*" (Meng et al. 2016). It consists of different application parts. The core application is Apache Spark, which can be extended with different libraries to a powerful data analytics engine. The different libraries are Spark SQL, Spark Streaming, MLib and GraphX.[2] Spark SQL adds interactive queries and Spark Steaming the handling of Streaming Data. The machine learning library of Spark MLib contains predefined machine learning algorithm like logistic regression or decision trees, but the number of algorithms is less than the number of algorithms in the popular machine learning library scikit-learn for python (Pedregosa et al. 2011). The GraphX library completes the Apache Spark Framework, but only allows to build "*graph from a collection of vertices and edges.*"[3]

For our research approach, Apache Spark is not useful, because it is not a native python framework but a framework written in scala with python bindings (Karau 2015, 9).

"*The Apache Hadoop software library is a framework that allows for the distributed processing of large data sets across clusters of computers using simple programming models. It is designed to scale up from single servers to thousands of machines, each offering local computation and storage.*"[4] The programming language for Hadoop is Java; this is not useful for our research (Lam 2010).

The last relevant project from the apache family is Apache Airflow (Kotliar et al. 2018). "*Airflow is a platform to programmatically author, schedule and monitor workflows.*"[5] As programming language python is used. But: "*Airflow is not a data streaming solution. Tasks do not move data from one to the other*

[2]https://spark.apache.org/.
[3]https://spark.apache.org/docs/latest/graphx-programming-guide.html#graph-builders.
[4]https://hadoop.apache.org/.
[5]https://airflow.apache.org/.

(though tasks can exchange metadata!)."[6] Thus is it not useful for our approach, because in the preprocessing tasks it is unavoidable to move the prepared data from one task to the next.

Besides the big software solutions from Apache, there are a few solutions like Celery, TaskTiger or Parsl which work native with Python and are available as Python packages.

"*Celery is an asynchronous task queue/job queue based on distributed message passing. It is focused on real-time operation, but supports scheduling as well. The execution units, called tasks, are executed concurrently on a single or more worker servers using multiprocessing.*"[7] Because of these key characteristics, Celery is of main interest for our research.

An alternative for Celery is TaskTiger, which is also a task queue. But the library is still in development and no major release is available (current version 0.10.1)[8] Therefore, it will not be used in this research.

Babuji et al. (2018) describe Parsl (Parallel Scripting Library)[9] in their paper. Parsl is a library that "*can be easily integrated into Python-based gateways*" (Babuji et al. 2018). This library allows a simple management and workflow scaling. Its main purpose is to "*manages the execution of the script on clusters, clouds, grids, and other resources*" (Babuji et al. 2018). It "*orchestrates required data movement; and manages the execution of Python functions and external applications in parallel*" (Babuji et al. 2018). The authors do not implement a web application but concentrate on the parallel execution of other programs. Furthermore, there is no example implementation and no description on how to distribute tasks in Parsl.

Lunacek et al. (2013) describe in their paper an approach about "*the scaling of many-task computing*" on cluster supercomputers (Lunacek et al. 2013). They compare the python libraries IPhython parallel and Celery. For their approach they evaluated both tools on a cluster. This is an interesting approach, but in our approach we are focusing on small settings like a laptop or a workstation as well as big settings like clusters.

Methodology

Here we will describe what kind of scaling options Python offers for the implementation of the data processing component of the web application. We will also describe which of these options we have implemented and what architectural choices we made. Finally we present the mathematical foundations we use to determine the scaling of the application.

[6]https://airflow.apache.org/.
[7]http://www.celeryproject.org/.
[8]https://pypi.org/project/tasktiger/.
[9]https://parsl-project.org/.

Handling the Data Processing in the Web Application

In order to share the resources of our computer between the web application and the processing of the date we receive from the data source, we need to discuss, which options Python provides to solve this issue. Furthermore, if the load on the computer to process the data becomes too high, we need to distribute the computations among different servers. Generally there are three options available:

- Implement the data processing in the same thread as the web application (i.e. single threaded approach).
- Use a concurrency model Python provides.
- Use distributed task queue to share the computation between multiple servers.

The Single Threaded Approach

This programming model is not recommended because the application can at any time either handle a web request or a data processing task but not both at the same time. Depending on how fast new data arrives and how computationally intensive the processing is, users may experience a noticeable delay in the handling of their web request.

Concurrency Models of Python

To determine which concurrency model is appropriate, we have to determine if the data processing tasks are CPU bound or I/O bound tasks.

A CPU bound task utilizes the CPU in long bursts with short waiting periods for I/O in between. An I/O bound task in contrast waits most of its execution time for I/O and utilizes the CPU in short burst (Tanenbaum and Bos 2014).

With this characterization we will see later in this article that the data processing tasks are almost always CPU bound.

The Python Standard Library offers the following concurrency models (Fein 2018):

- The ***threading*** library provides thread-based parallelism for Python.
- Process-based parallelism is provided by the ***multiprocessing*** library.
- With the ***asyncio*** library it is allowed to write single threaded concurrent code.
- Finally the ***concurrent.future*** library enables us with a high-level interface for asynchronously executing callables.

Thread-based Parallelism

The threading model in Python is severely restricted because of the *global interpreter lock (GIL)* (Wouters 2017). Due to this lock Python cannot fully utilize

a multiprocessor/multicore system. Two different threads in Python can't run two instructions simultaneously because the interpreter has to acquire the GIL before the execution of each command. Hence multithreading in Python is helpful, if the tasks you wish to parallelize are I/O-bound.

Therefor this parallelism model has to be rejected for our usecase, because it would not help the data processing tasks to scale and use the full capacity of a multiprocessor/multicore system.

Process-based Parallelism

This kind of parallelism has the advantage, that for each process a new Python interpreter is started and each interpreter has its own GIL. Because of this, the full capacity of a multiprocessor/multicore system can be reached by starting as much processes as there are processors respectively core in the processors.

Process-based parallelism is therefore useful in situations where CPU-bound tasks have to run in parallel. Hence we will use this method to research its scaling behavior in the application.

Asynchronous I/O

> ***asyncio*** is used as a foundation for multiple Python asynchronous frameworks that provide high-performance network and web-servers, database connection libraries, distributed task queues, etc.
> ***asyncio*** is often a perfect fit for IO-bound and high-level structured network code.[10]

This characterization also excludes this technique from the scope of this research.

The Concurrent.future Library

This library provides the ***ProcessPoolExecutor*** class which enhances the ***mutiprocessing*** library. It starts a pool of processes, manages the communication between the main process and the processes in the pool and starts tasks in the processes of the pool.

As this is exactly the same feature we would have implemented for the execution of the data processing tasks, we will use this class when we examine process-based parallelism for our application.

Distributed Task Queues in Python

In the Python ecosystem ***Celery*** (Solem and contributors 2019) is the defacto standard for distributed task queues. Furthermore Django supports Celery out of the box since Celery version 3.1.[11]

[10]First and second paragraph: quote from *https://docs.python.org/3/library/asyncio.html.*
[11]See *http://docs.celeryproject.org/en/latest/django/first-steps-with-django.html.*

Celery itself needs a message broker which distributes the tasks from the web application to the worker processes on other servers. The Celery documentation recommends ***RabbitMQ*** (Pivotal Software Inc. 2019) or ***Redis*** (Sanfilippo and contriburors 2019) as message broker.

From this two message brokers RabbidMQ is the more powerful one (regarding its features and configuration possibilities). Unfortunately this is a disatvantage for our approach because we want to develop an application that needs as less additional knowledge outside of the Python ecosystem as possible.

In contrast Redis is easy to install and needs no further configuration for our purpose. Therefore, we use Redis as message broker for Celery in our application.

Architecture

After the discussion of the theoretical fundamentals for multiprocessing and distributed task queue with Celery the key results were used to develop the following two different architecture models. Both architecture models need to fulfill the following requirements:

- fast and consisting processing of big amount of data
- possibility for flexible scaling
- after initial configuration a comfortable configuration
- no integration of third-party software, only python libraries are allowed
- possibility to connect different data sources
- avoid data lost
- flexible output of the result data
- both architectures should be integrated in one application

Multiprocessing

The architecture of multiprocessing contains different components. The data sources can be messages from a MQTT broker, data from a special time series database for sensor data (Burdack et al. 2018), data from a PostgreSQL database, collection of csv-files and so on. For multiprocessing it is not necessary that this data is static, it is also possible to work with streaming data.

The input data – static or streaming data – will be collected in the buffer area in buckets. Each of these buckets contains a predefined number of input data. If this count of input data in the buffer is reached, the whole data package is sent to the preprocessing app. The idea behind the buffering is to provide a method to reduce the arrival rate in the app at the cost of increasing the service time.

The preprocession (web-) app as well as the multiprocessing pool are parts of the same host system. This host system defines the maximum count of workers for the multiprocessing pool depending on the count of processors resp. cores.

The number of workers for the multiprocessing pool in this approach is defined by the preprocessing app. If no limitation will be given, the host system in theory can take the whole available count of cores for the workers.

The data package which will be sent to the preprocessing app enters the multiprocessing pool. There the processing rules which are defined in the chained task in the preprocessing app will be applied to the input data.

The result of this modification will be sent as one data package to the result interface. The result interface can send these result data to for instance a Bokeh plots, other application for example a machine learning platform or to other host system for further modifications. The whole procedure is presented in Figure 1.

Figure 1. *Multiprocessing Architecture*

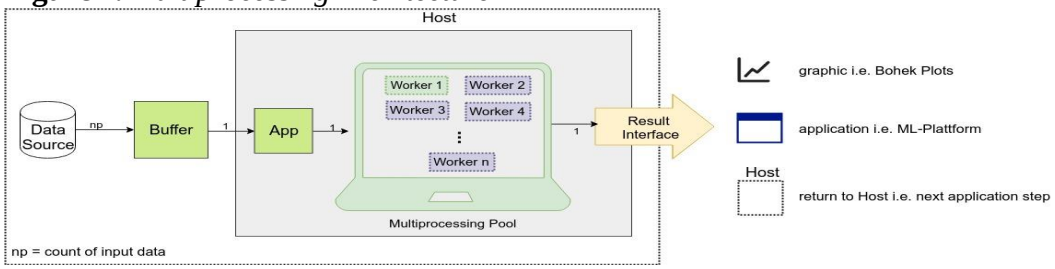

Source: Authors.

The multiprocessing pool works with a special chained task, shown in Figure 2, which is only proceeded on one worker. The defined package of input data discussed below are json files, which are be compressed and base 64 encoded to reduce the bandwidth and avoid string encoding problems in python. This transformed data package is the input data for the chained task.

The chained task starts with the prepare task, which decodes the data and transforms the raw data into a pandas data frame. This panda data frame is the basis for the processing in the further tasks. All the different defined tasks are based on working with pandas data frames for high-performance data manipulation.

Based on the configuration in the preprocessing app, a specific number of subtasks (Task 1 - Task n) have to be processed. The output of each task will be used as the input of the following task. If the last task is finished, the result data frame is passed to the result task.

The result task prepares the data frame for the further working as noted above for example for other applications. The subtasks are monitored and scheduled by a scheduler, which looks after the right execution of the tasks in the right order.

In the multiprocessing approach all the subtasks are executed in the same worker process. No data has to leave the worker process in order to pass the data to the next subtask.

Figure 2. *Chained Task in the Multiprocessing Architecture*

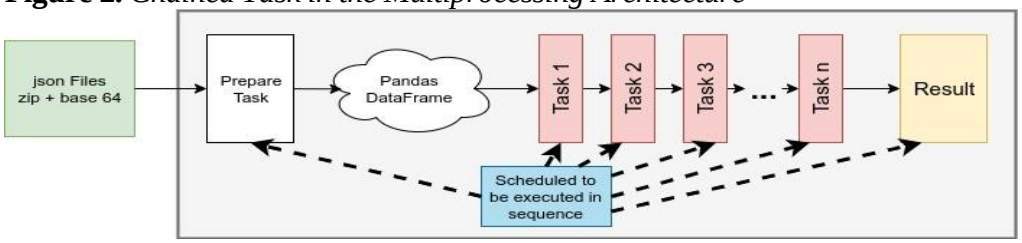

Source: Authors.

Distributed Task Queue

The architecture of the distributed task queue with Celery is in contrast to multiprocessing more complex. The data source is the same as describe in multiprocessing above. Here it is also possible to work with different kinds of data sources like streaming or local data. The input data will also be collected until a predefined count of input data in the buffer. The whole collected data package will be sent to the host system, which only contains distribution components of Celery and the preprocessing application. But the data will be not transformed on the host system itself, the data package will be passed on to Redis, which manages the Celery workers on the different worker nodes.

These worker nodes transform the data with the preprocessing rules, which are defined in the application.

If all subtasks are done, the result is passed to the result interface. This result interface can be the same as described in multiprocessing. The whole procedure is shown in Figure 3.

Figure 3. *Celery Architecture*

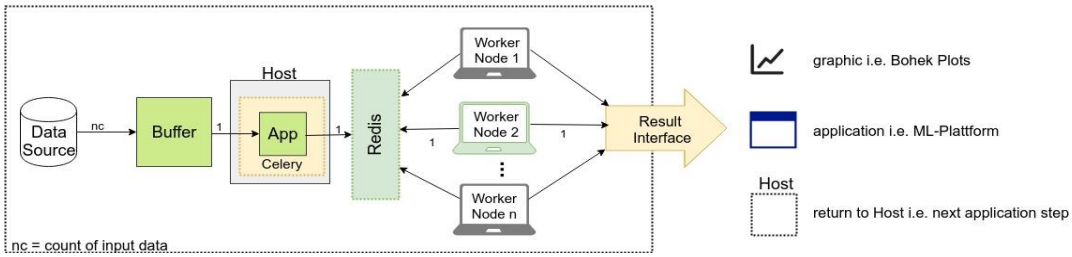

Source: Authors.

The distributed task queue with Celery works with a special chained task, which is visualized in Figure 4.

Figure 4. *Chained Task in the Distributed Task Queue Architecture*

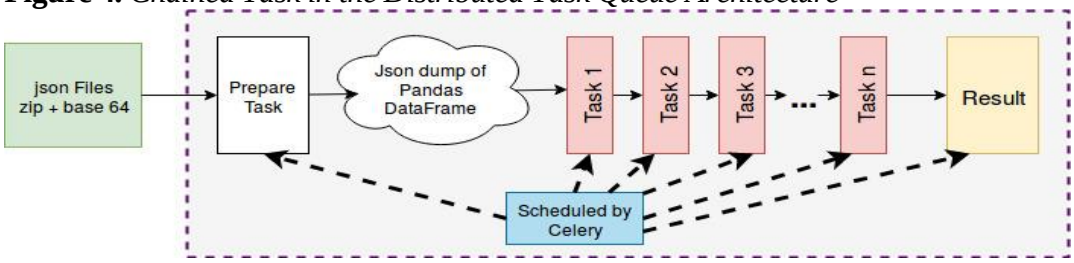

Source: Authors.

In contrast to the multiprocessing architecture, Celery provides the scheduling and subtask chaining (i.e. use the output data of a previous task as input for the next task) out of the box.

Furthermore, Celery distributes the subtasks round robin to the worker processes on the worker nodes. That makes it necessary to exchange the data via Redis among the subtasks. Unfortunately pandas data frames cannot directly be transported via Redis. Therefore we first had to convert the result of a subtask into

a json representation of the pandas data frame, then send it via Redis to the next subtask and convert it back to a pandas data frame.

This conversion before exchanging data is the reason we introduced the buffer component in the first place. It allows us to reduce the number of conversions per data row significantly.

Application of Queueing Theory

Finally we need a tool to help us to determine how to scale our application. It should consider the following point:

- The arrival rate of the data.
- The tasks chained together to process the data (see Figures 2 and 4).
- The number of worker processes that run the chained task on the data.

This tool can be found in the mathematical field of Queueing Theory by applying the following:

A queue with c servers is ***stable*** (will not grow without bound) if the following inequality holds:

$$\rho = \frac{\lambda}{c\mu} < 1$$

Where ρ is the server utilization, λ is the arrival rate and μ is the service rate (the inverse of the service time for one task) (Bhat 2015).

Assigning the Components of this Inequality to our Application

We will show how the variables c, λ and μ must be applied to our problem, in order to determine the server utilization ρ.

The First Component is the Number of Server c

In this context **server** denotes the consumer of the data not the physical computers in our server room.

To explain this term for our purpose, we have to distinguish between the multiprocessing architecture and the distributed task architecture.

Multiprocessing Architecture

In this case c is the number of worker processes in the process pool (see Figure 1). Additionally this number may not exceed the number of processor cores minus one. This spare core is used to serve the http requests to the application. The others are used for the data processing. It is important to not exceed the number of

cores on the system because the data processing tasks are CPU-bound. If the number of workers is bigger than the number of available cores, then the data processing tasks have to wait for previous tasks to finish.

Distributed Task Queue Architecture

Here c is the number of all the worker processes summed over all worker nodes (see Figure 3). Analog to the multiprocessing case the number of worker processes per worker node should not exceed the number of processor cores on the respective node.

The Second Component is the Arrival Rate λ

The arrival rate denotes how fast new data is ready to be processed, for example, how often a sensor value is read in a given time interval.

We have to distinguish two different arrival rates, depending on where we measure them:

λ_{ds} The arrival rate of the data rows measured at the data source.

λ_{buf} The arrival rate of the buffered data rows (messages) measured after the buffer.

If the buffer puts n data rows in one message then the following equation holds:

$$\lambda_{ds} = \lambda_{buf} \cdot n$$

The Third Component is the Service Rate μ

This is the inverse of the time the data processing task takes to calculate its result for a given data row or a buffered message depending on which arrival rate was chosen (see Figures 8-9).

To calculate μ for the chained task, you should sum over the service time of all the tasks that form the chained task and take the inverse of it.

The Final Component is the Server Utilization ρ

It is the percentage of the utilization of the maximal amount of the computing power of the complete system.

A positive value much smaller than one, denotes that the system could process more data without problems. A value very close to one means, that you use the complete computation power of the system without stalling the output. And a value of one or greater, shows, that your tasks require more computation power than the one your system can provide. In this case the queue with

unprocessed data grows faster than it can be consumed and the system becomes unstable. The concrete application of this inequality will be discussed in the findings section.

Findings

The Preprocessing App

Through the architecture of the web framework from Django (Vincent 2018), it is possible to integrate other python modules like MQTT module or database connection modules. This main program structure allows, to implement the process components for multiprocessing and task queue in the same application. Through a simple configuration setting in the app the method can be selected. Through this possibility, no third part integration of other programs are necessary. This leads to an easy managed application, which only depends on python and its modules.

The main purpose of this approach is not the visualization of the weather data. The main purpose is to implement both different methodologies as explained before in one application. For this reason, a preprocessing application was developed, which allows to configure and to monitor flexible preprocessing tasks in an easy way. By using a project management system, it is possible to configure and to store different preprocessing tasks settings in a project. Each project consists of the following components:

description: a unique name for identification
mqtt broker: information about the used mqtt broker
mqtt client: information about the mqtt client information
topic: name of the topic, where the data should be subscribed
task: the defined chained task
method: working method (task queue or multiprocessing)
buffering factor: count input data in buffer
arrival rate: time difference between data points to arrive in the buffer
worker count: count of used workers

Figure 5 shows the project overview of the *Preprocessing App*. This view is the central point of the *Preprocessing App*. There is an overview about all created projects, where it is possible to go into detail for each project. It is also possible to start and stop the preprocessing for a selected project.

Web sites have a high risk of security issues, especially if they contain input fields. One of the most common issues is cross site scripting. In the background of the industry 4.0 cross site scripting issues (Stock et al. 2017) are most expensive for companies that use web technology especially in their production environment. Each security gap leads to expensive consequences and if it takes a long time to less trust in new technologies. To avoid this risk, the templates from the *Preprocessing App* were tested with the methods of Stigler et al. (2018) to detect cross site scripting vulnerabilities in websites. All implemented templates are now guarded against cross site scripting attacks.

Figure 5. *Preprocessing App Project Overview*

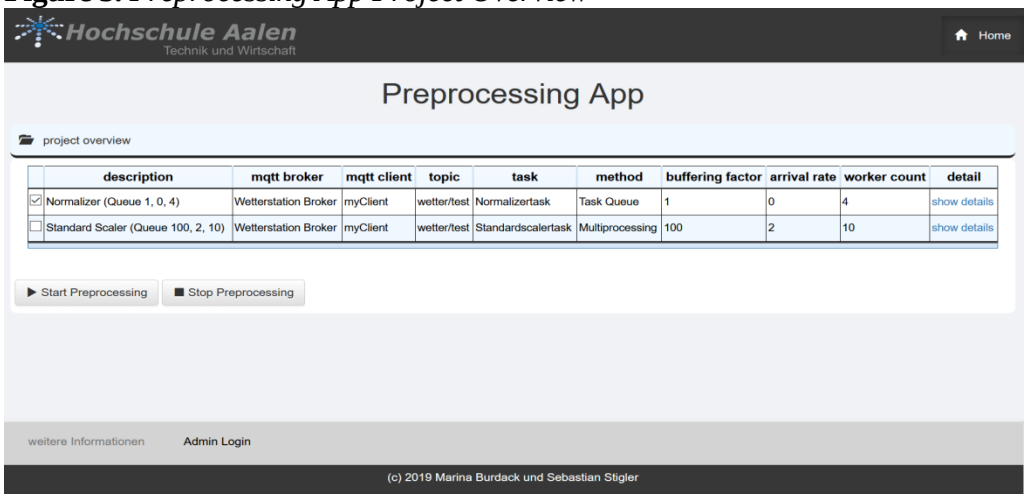

Source: Authors

Figure 6 shows the web template to create new projects over the admin panel from the web application. All input fields are checked for cross site scripting vulnerabilities with the tests from Stigler et al. (2018). The report shows that the *Preprocessing App* is protected against the most common security flaws.

Figure 6. *Add New Project*

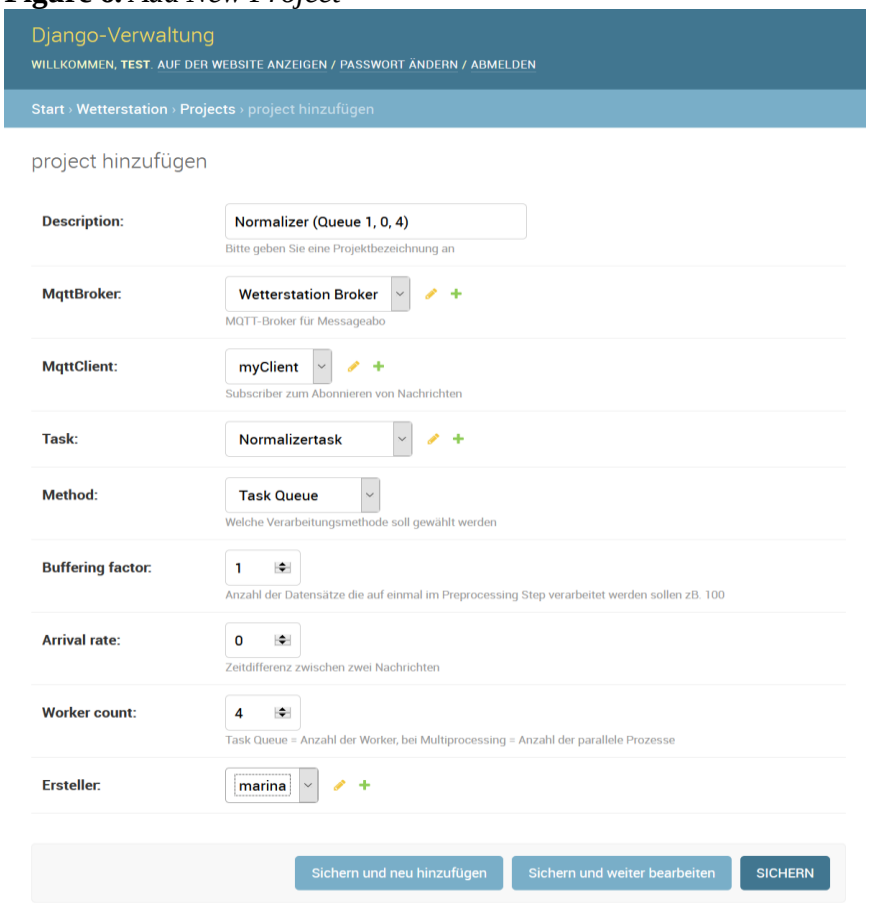

Source: Authors.

Evaluation Data

The test data set consists of real-time sensor data from the Davis weather station of the Aalen University (*http://wetter.infotronik.htw-aalen.de/*). This weather station publishes one new message every minute by a MQTT client. Each message consists of a json – structure which contains 26 numerical values like wind speed, outdoor temperature, barometer and seven values as strings, for example the wind direction. A MQTT Broker - in our case mosquitto MQTT - manages this data under the topic "'wetter"`. To store these messages another MQTT client subscribes the topic and stores each message as one data row in a Postgres database. At the end of the data collection process the test data set contained 750,000 data rows.

These 750,000 data rows were then packed in different bucket sizes: 1, 10, 100, 1000, 3000, 5000, 7500 and 10000 rows/message.

From now on ***row*** or ***data row*** denotes a single data package directly out of the data source. When we talk about a ***message*** we mean a single data package after the buffering component. A ***message*** contains several ***data rows***. The amount is determined by the buffering factor.

For real-time testing, we send the messages from these datasets without delay to the application.

Preprocessing Tasks for Evaluation

In contrast to the prepare task the duty of the result task depends on what you want to do with the result afterwards: the data could be transformed into a different, converted into a graphic or sent to another application. Therefore in the evaluation this task is only implemented as a dummy task which receives the data and does nothing with it.

Beside these tasks, 14 different classical preprocessing tasks will be implemented in the application. The first six tasks are methods directly from the modern data science library for python, pandas (McKinney et al. 2019). These methods are:

- abs
- aggregated sum
- drop duplicates
- handling missing
- fillna_mean
- fillna_median
- fillna_zeros

In addition eight tasks are implemented from the scikit learn library (Pedregosa et al. 2011, Cournapeau and contriburors 2019). These tasks consist of:

- max_abs_scaler
- min_max_scaler_0_1

- min_max_scaler_m1_1
- normalizer
- quantil_tranformer_normal
- quantil_transformer_uniform
- robust_scaler
- standard_scaler

Evaluating the Service Times for the Various Subtasks and Applying of Queueing Theory

We used a Server from Nvidia for the evaluation with the following specifications:

Nvidia DGX-Station
CPU Intel Xeon(R) CPU E5 2698 v4 @ 2.20GHz x 40[12]
RAM 256 GB
SSD 6TB

In the methodology section we provided an inequality to determine under which circumstances the application processes the data without blocking.

An important part of this inequality is the service time μ^{-1}. To determine the service time of each of the preprocessing task we used the following procedure:

1. Choose 75 messages from each bucket of our evaluation data.
2. Send a message to be processed by the chosen task and execution method (single threaded, multiprocessing and distributed task queue).
   Measure the execution time.
3. Repeat until all messages where processed.

We use the single threaded approach to get the pure execution time of the task without any overhead from the multiprocessing resp. the distributed task queue approach.

This overhead in the multiprocessing case is the sending of the data from the main process to one of the worker in the worker pool and the time it takes to send the result back. In the case of the distributed task queue the overhead contains the sending of the serializes pandas data frame to the worker node via Celery (with the help of Redis) and the deserialization back to a pandas data frame so that the task can do its job. Furthermore the result must be serialized as well and then sent, via the Celery infrastructure, back to the main process.

As you can see, the overhead of the distributed task queue per message is higher than the overhead of the multiprocessing approach. And so the old proverb "*There is no such thing as free lunch*" is again confirmed. If you want to increase the processing power of your system by switching from multiprocessing to a distributed task queue, you have to pay with an increased transportation time of the

[12]20 physical Cores (40 with Hyper Treading).

data. We will later show how to tune the system to compensate this increase in the overall service time.

Figure 7 shows the result of the evaluation procedure from above, applied to the ***prepare*** task, run in single threaded mode. The first column shows the size of the messages. For example the last row indicates the test set where each of the 75 messages contains 10000 data rows. A row contains the mean (depict with ø) and the standard deviation (depict with σ) of the service time for the processing of the whole message in μs and the service time per data row.

Figure 7. *Table of Single Threaded Approach for the Task_Prepare (Henceforth known as **Base Line**)*

	duration/msg		duration/row	
rows/msg	ø	σ	ø	σ
1	3840.881	453.105	3840.881	453.105
10	4019.249	217.332	401.925	21.733
100	5951.921	413.597	59.519	4.136
1000	23652.684	1825.831	23.653	1.826
3000	63629.374	5091.716	21.210	1.697
5000	103221.863	8230.345	20.644	1.646
7500	156601.112	12795.871	20.880	1.706
10000	207001.974	15776.564	20.700	1.578

Source: Authors.

Figures 8 and 9 show the result of this evaluation of all preprocessing tasks. Each subplot has logarithmic x and y axis. The x axis denotes the number of data rows per message. In Figure 8 the y axis is the service time per message in μs and in Figure 9 it is the service time per data row in μs.

Each subplot shows a graph for the base line, the multiprocessing variant and the task queue variant. It can easily be seen, that using the base line offers the best service time, followed by multiprocessing and the task queue approach offers the worst service time. This disadvantage can be compensated by the fact, that multiprocessing can use more than one CPU core to process tasks in parallel compared to the base line implementation; but it can only use the cores on one single physical computer. A task queue can spread the tasks over all the cores on multiple computers.

The dark grey stripe on the right of each subplot denotes a region where the slope of each curve increased significantly. This happened because the processing of the task with such a large message reaches (or at least is near) the limits of the CPU. You should avoid using messages of this size.

Figure 8 shows, that up to $100\,\frac{rows}{msg}$, the service time per message, stays roughly the same. The time doubles at most while the number of rows per message grows by a factor of a hundred. And in the interval from 1 to $1000\,\frac{rows}{msg}$ the time increases by a factor less than 10. Therefore the length of message has not a very high impact on the time to process it.

Figure 9 shows the advantage of buffering more data rows into a single message to process it in one go: In a message with many data rows, the service time for each data row in it decreases significantly.

Figure 8. *Mean Service Time per Message*

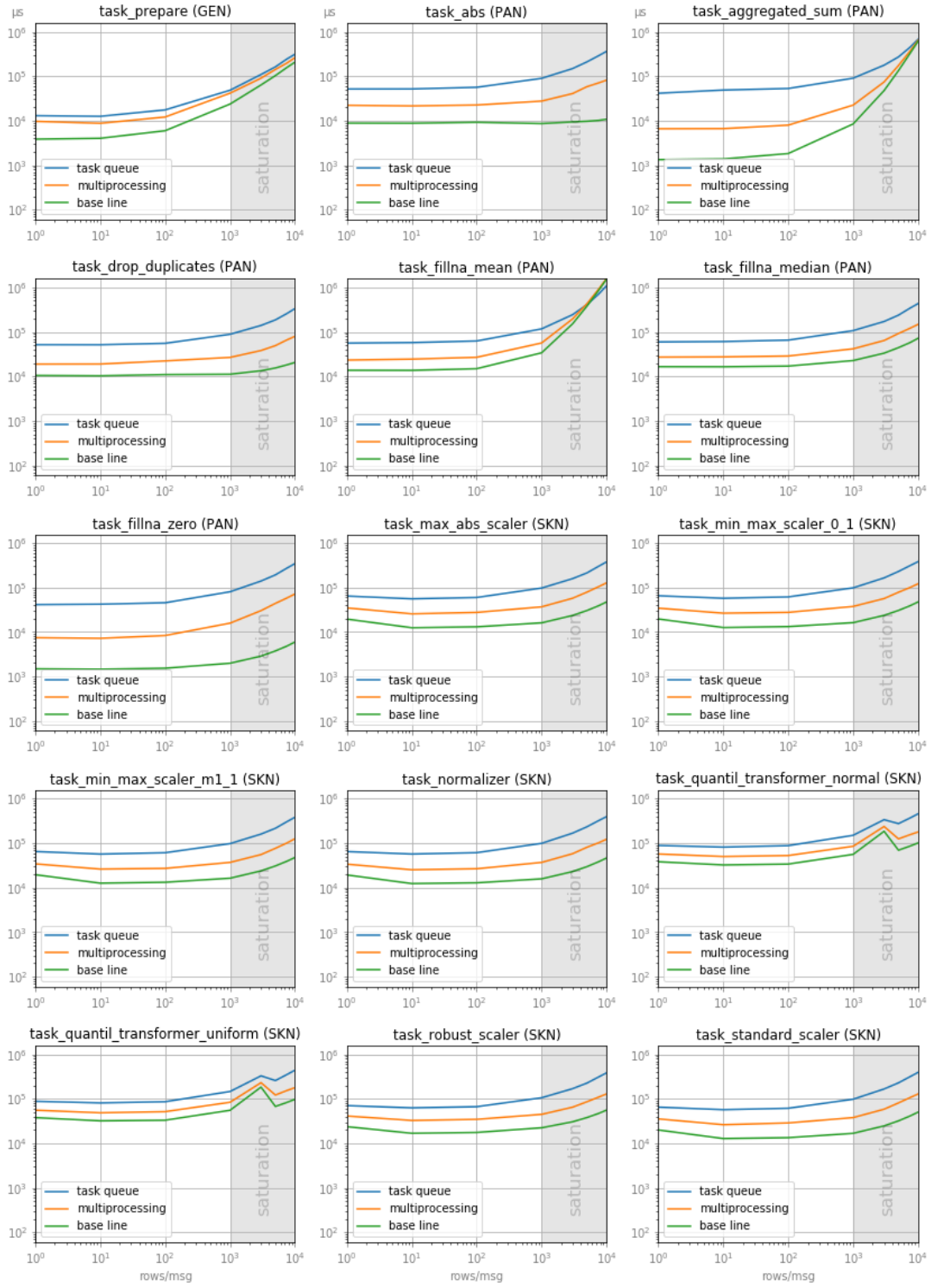

Source: Authors.

Figure 9. *Mean Service Time per Row*

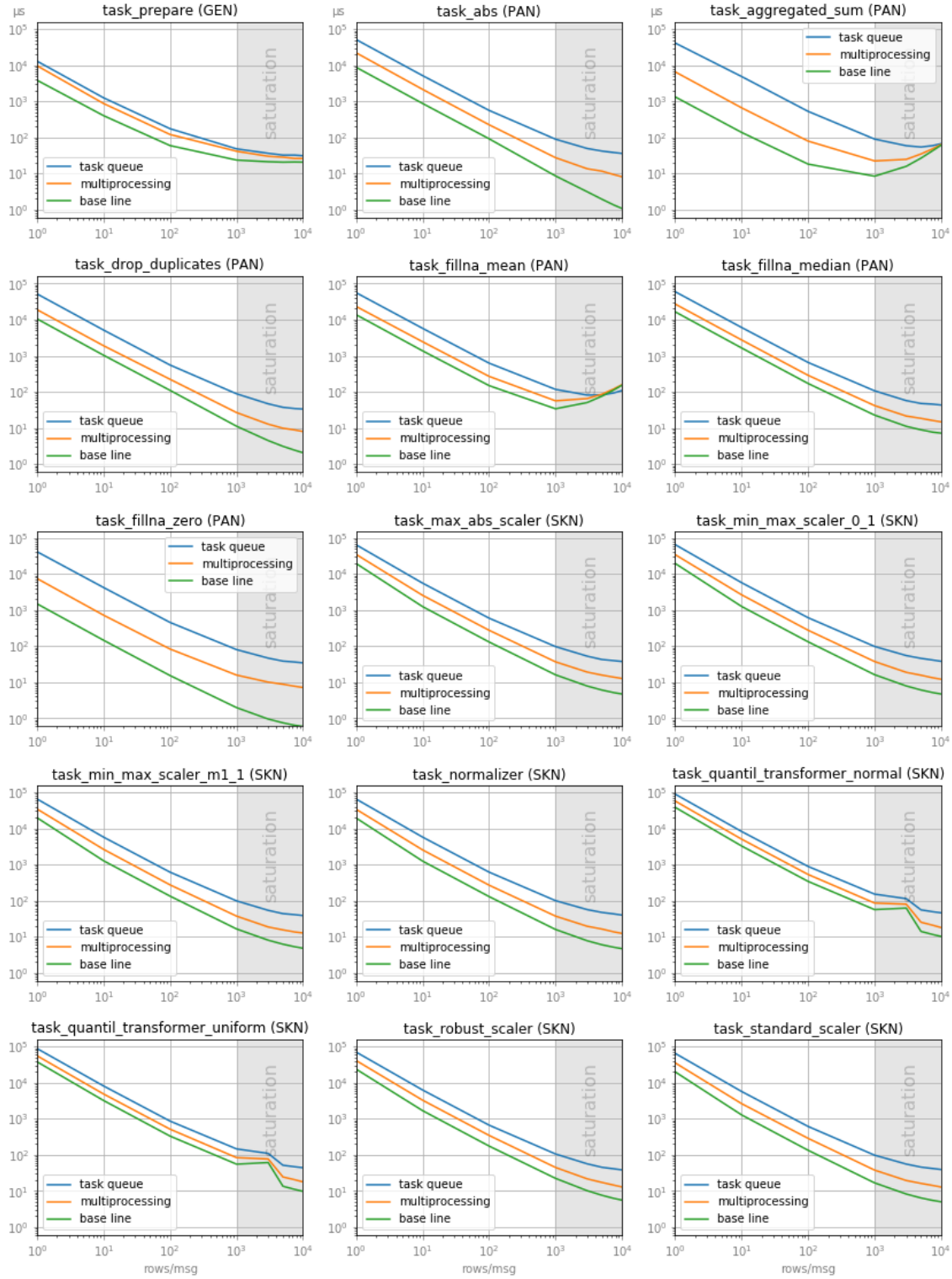

Source: Authors.

Discussion

How can we Use this Data to Scale our Application Properly

For the purpose of this example calculation we assume that there are neither restrictions on an acceptable arrival rate nor constraints regarding the delay the buffering will introduce to the system by waiting until the predefined number of data rows were received from the buffer before sending a message into the application.

How to Keep the Service Time Constant while Switching from Multiprocessing to Task Queues?

Assume you use the task_fillna_zero task and use no buffering in multiprocessing mode. If you look in Figure 9 at the subplot of this task you can see, that its service time for multiprocessing is approximately $7ms$. On the curve for the task queue, in the same subplot, you get this service time if you buffer with approximately 6 rows per message.

What can be Done if the Arrival Rate Increases but the Service Time should Kept the Same in a Task Queue?

In this case you can use the inequality for the server utilization ρ. If you increase the arrival rate by the factor of n then the number of services c has to grow with the same factor.

How to Use the Information from Above to Determine Good Parameter for a Given Chained Task?

In the central subplot of Figure 10 we show the mean service time per data row of the following chained task[13] (with the approximate service times at a buffer factor of 10 on a task queue):

1. task_prepare $\mu_p^{-1} \approx 1.3ms$
2. task_fillna_zero $\mu_f^{-1} \approx 4.2ms$
3. task_normalizer $\mu_n^{-1} \approx 5.7ms$
4. task_drop_duplicates $\mu_d^{-1} \approx 5.1ms$

The complete chained task should therefore have a service time of approximately $16.3ms$.

[13]We ignore the service time for the task_result in this example as we don't want to use the processed data afterwards! In a real application, the service time for the task_result must be added, too.

Now we will use the inequality for the server utilization to calculate an arrival rate, with respect to a stable system ($\rho < 1$). In the beginning of this section we specified our test server as a server with 20 CPU cores, therefore we use $c = 20$ in the inequality. As we used service time **per data row**, we want to calculate λ_{ds} (the arrival rate measured at the data source).

$$\lambda_{ds} < c\mu = 20 \cdot \frac{1}{16.3ms} = 1226.99Hz$$

To determine the delay between two consecutive data rows we need to build the inverse of λ_{ds}:

$$\lambda_{ds}^{-1} > \frac{1}{1226.99Hz} = 815\mu s$$

To be on the save side, we will use $\lambda_{ds}^{-1} = 900\mu s$.

Figure 10. *Mean Service Time per Data Row of the Above Chained Task (The left subplot shows the result, when the data rows are sent with no delay[14] to the chained task. The central plot shows the sum of subplots in Figure 9 that forms the subtasks of the chained task. The right subplot is the result of the test run with* $\lambda_{ds}^{-1} = 0.0009s$*).*

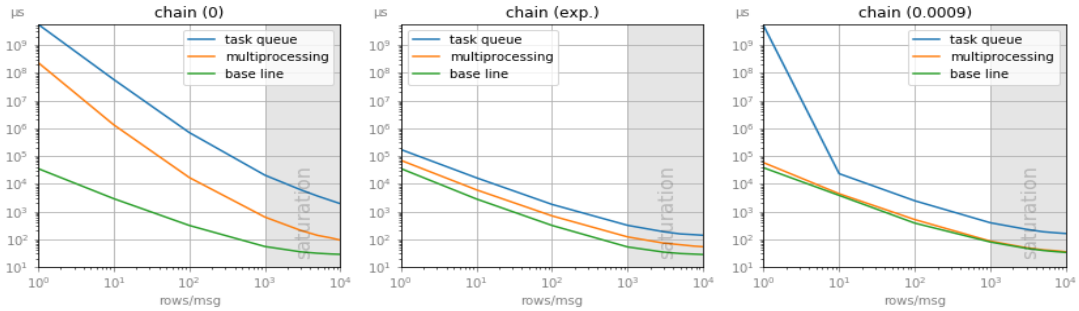

Source: Authors.

The data for the left and right subplot of Figure 10 was created by sending the complete evaluation data without delay to the application on the DGX-Station, i.e. we send 750,000 data rows in bucket from 1 row per message up to 10000 rows per message to the chained task.

In subplot "chain (0.0009)"' of Figure 10 the base line matches the prediction in "chain (exp.)" quite nicely. The service time for the multiprocessing is even a bit better than the prediction. The graph for the task queue shows that the prediction from $10\frac{rows}{msg}$ onwards are a bit worse than the prediction. For the $1\frac{rows}{msg}$

[14]We measured $4\mu s$ between any two consecutive data rows.

entry we see a very high value for the service time. But this is ok as we calculated the arrival rate based on the values of the task queue at $10\frac{rows}{msg}$.

To verify whether we produced a stable configuration, we have to calculate the server utilization corresponding to the plots in Figure 10.

Figure 11. *Server Utilization (The first three columns show the utilization of the chained task for the base line (bl), the multiprocessing (mp) and the task queue (tq) variant of the software while serving new data rows with no delay. The three columns in the middle show the expected utilization with $\lambda_{ds}^{-1} = 0.9ms$, $c = 20$ for multiprocessing and task queue and $c = 1$ for the base line[15] and the service time according to the summed service time of the above named tasks depicted as in the central subplot of Figure 10. The last three columns show the actual run of this chained task on the DGX-Station Server).*

	chain (0)			chain (exp.)			chain (0.0009)		
rows/msg	bl	mp	tq	bl	mp	tq	bl	mp	tq
1	8756.157	2897599.497	69401701.487	39.026	3.872	9.474	41.771	3.191	275433.419
10	723.311	16593.341	712226.313	3.127	0.334	0.907	4.209	0.242	1.277
100	78.269	208.676	8716.986	0.348	0.039	0.100	0.423	0.028	0.135
1000	13.629	7.847	254.033	0.058	0.007	0.018	0.088	0.005	0.022
3000	8.736	2.578	74.856	0.038	0.004	0.010	0.052	0.003	0.013
5000	7.773	1.712	44.746	0.034	0.004	0.009	0.044	0.002	0.010
7500	7.317	1.388	30.874	0.032	0.003	0.008	0.039	0.002	0.009
10000	7.099	1.153	23.754	0.031	0.003	0.008	0.037	0.002	0.009

Source: Authors.

It can be seen, that the ρ values for all implementation types of the prediction (central three columns) in the $1\frac{rows}{msg}$ as well as the base line value for $10\frac{rows}{msg}$ should lead to instabilities as the ρ values are strictly greater than one. All other entries indicate that the resulting run should lead to stable executions of the chained task. Although the 90.7% utilization for the task queue at $10\frac{rows}{msg}$ should lead to a stable process, as Figure 11 shows, the task queue performs a little worse than predicted, which actually leads to an instable process.

If we compare our expectations with the actual runs (three rightmost columns) we see, that with the exception of the $10\frac{rows}{msg}$ all predictions hold.

We suspect, that the utilization of the network connection to the worker node may be the reason for the results of the task queue. The reason for this assumption lies in the construction of the data for Figure 9: We sent one message and then measured the time until the result was ready before we sent the next message. For the calculation of the task queue values for Figure 10 "chain (0.0009)" we sent the messages with a constant rate of $1111{,}11Hz$ ($\frac{1}{900ms}$) over the network to the worker node.

Finally we have to discuss the leftmost subplot of Figure 10 resp. the three leftmost columns of the table in Figure 11.

[15]The base line is a single threaded implementation in Python. Hence only one core can be used (Python Software Foundation 2019).

Here we want to show how an instable process may look like. The slope of the multiprocessing and the task queue graph in Figure 10 “chain (0)” is much steeper than the slope of the base line. In contrast, the slopes in “chain (exp.)” of the three graphs are very similar and when compared to the stable parts of the graph in “chain (0.0009)” it can be seen, that the slops in this areas are similar too. The values in the table in Figure 11 show, with ρ values much greater than one, that the graphs actually show instable processes.

Some Advice on Choosing the Architecture for your Own Application

The inequality for the server utilization can help you to determine the number of servers c so that the system stays stable.

If c is less or equal to number of cores on the host server then multiprocessing should be used.

If c exceeds the number of cores on the host system then it is advisable to use a distributed task queue with at least c task queue worker processes.

Conclusions

This article demonstrated how far you can get in a data processing application with Python libraries only. Furthermore, it was demonstrated that even if Python has its flaws in puncto utilization of more than on core per process (Python Software Foundation 2019), it is possible to write an application that circumvented this problem by using multiprocessing or even a distributed task queue to utilize more than one server for the data processing.

The architecture of the application for the multiprocessing and the task queue approach was presented and it was shown how to organize a data processing task that is built from some basic data processing tasks and how to chain them together.

An essential part of this article was the use of queueing theory to explain how to scale an application that works as a data processing pipeline.

In the findings section, it was described how the application works and the evaluation of the performance of the two aspects of the application (the multiprocessing and the task queue aspect) was discussed.

Finally, it was concluded that the restriction to typical preprocessing tasks was not as severe as it seems. The techniques to determine the utilization of a server can be directly applied to machine learning tasks and post processing task like visualization.

References

Babuji YN, Chard K, Foster IT, Katz DS, Wilde M, Woodard A, Wozniak JM (2018) *Parsl: scalable parallel scripting in python*. 10th International Workshop on Science Gateways, 13-15 June 2018.

Bhat UN (2015) *An introduction to queueing theory. Modelling and analysis in applications*. Basel: Birkhäuser.

Borthakur D, Gray J, Sarma JS, Muthukkaruppan K, Spiegelberg N, Kuang H, … Aiyer A (2011) Apache hadoop goes realtime at facebook. In *Proceedings of the 2011 ACM Sigmod International Conference on Management of Data*, 1071-1080. New York, USA: ACM.

Burdack M, Rössle M, Kübler R (2018) A concept of an in-memory database for iot sensor data. *Athens Journal of Sciences* 5(4): 355-374.

Burdack M, Rössle M (2019) A concept of an interactive web-based machine learning tool for individual machine and production monitoring. In *Intelligent Decision Technologies*, 183-193. Singapore: Springer Singapore.

Cournapeau D and contriburors (2019) *Scikit-learn 0.20.3*. Retrieved from https://scikit-learn.org.

Fein P (2018) *Concurrency*. Retrieved from https://wiki.python.org/moin/Concurrency.

Kaggle, Crawford C, Montoya A, O'Connell M, Mooney P (2018) *2018 kaggle ml & ds survey. The most comprehensive datdata available on the state of ml and data science*. Retrieved from https://www.kaggle.com/kaggle/kaggle-survey-2018.

Karau H (2015) *Learning spark - lightning-fast big data analysis*. Sebastopol: O'Reilly Media, Inc.

Kotliar, M., Kartashov, A., & Barski, A. (2018). CWL-airflow: A lightweight pipeline manager supporting common workflow language. *bioRxiv*, 249243.

Lam C (2010) *Hadoop in action* (1st Edition). Greenwich, CT, USA: Manning Publications Co.

Lunacek M, Braden J, Hauser T (2013) The scaling of many-task computing approaches in python on cluster supercomputers. In *2013 IEEE International Conference on Cluster Computing*, 1-8. https://doi.org/10.1109/CLUSTER.2013.6702678.

McKinney W, Augspurger T, Ayd W, Bartak C, Battiston P, Cloud P, … Young G (2019) *Pandas. Python data analysis library v0.24.2*. Retrieved from https://pandas.pydata.org/.

Meng X, Bradley J, Yavuz B, Sparks E, Venkataraman S, Liu D, Freeman J, Tsai DB, Made M, Owen S, Xin D, Xin R, Franklin MJ, Zadeh R, Zaharia M, Talwalkar A (2016) Mllib: Machine learning in apache spark. *The Journal of Machine Learning Research* 17(34): 1-7.

Pedregosa F, Varoquaux G, Gramfort A, Michel V, Thirion B, Grisel O, Blondel M, Prettenhofer P, Weiss R, Dubourg V, Vanderplas J, Passos A, Cournapeau D, Brucher M, Perrot M, Duchesnay É (2011) Scikit-learn: Machine learning in python. *The Journal of Machine Learning Research* 12: 2825-2830.

Pivotal Software Inc. (2019) *RabbitMQ*. Retrieved from https://www.rabbitmq.com/.

Python Software Foundation and JetBrains (2018) *Python developers survey 2018 results*. Retrieved from https://www.jetbrains.com/research/python-developers-survey-2018.

Python Software Foundation. (2019) *Thread state and the global interpreter lock*. Retrieved from https://docs.python.org/3/c-api/init.html#thread-state-and-the-global-interpreter-lock.

Rössle M, Kübler R (2017) Quality prediction on die cast sensor data. In *ATINER's Conference Paper Series*, number: COM2017-2272. Athens: ATINER.

Sanfilippo S and contriburors (2019) *Redis 5.0.4*. Retrieved from https://redis.io.

Solem A and contributors (2019) *Celery: Distributed task queue 4.3.0*. Retrieved from http://www.celeryproject.org.

Stigler S, Karzhaubekova G, Karg C (2018) An approach for the automated detection of xss vulnerabilities in web templates. *Athens Journal of Sciences* 5(3): 261-280.

Tanenbaum AS, Bos H (2014) *Modern operating systems* (4th Edition). Upper Saddle River, NJ, USA: Prentice Hall Press.

Van der Stock A, Smithline N, Gigler T (2017) *OWASP top 10 - 2017. The ten most critical web application security risks*. Retrieved from https://bit.ly/2qK2CcE.

Vincent WS (2018) *Django for beginners. Build websites with python & django*. SMTEBOOKS.

Vinjumur JK., Becker E, Ferdous S, Galatas G, Makedon F (2010) Web based medicine intake tracking application. In *Proceedings of the 3rd international conference on pervasive technologies related to assistive environments*, 37:1-37:8). New York, USA: ACM.

Wirth R, Hipp J (2000) CRISP-dm: Towards a standard process model for data mining. In *Proceedings of the fourth international conference on the practical application of knowledge discovery and data mining*, 29-39. Retrieved from https://bit.ly/2ONx0e7.

Wouters T (2017) *GlobalInterpreterLock*. Retrieved from https://bit.ly/2OMEo9I.